UNIVERSITY OF BRITISH COLUMBIA
VU UNIVERSITY AMSTERDAM

MASTER THESIS

Modeling the Appearance and Spread of Drug-Resistant Influenza

Author:
Judith Bouman

Supervisors:
Prof. dr. Daniel Coombs
(UBC) &
Dr. Robert Planqué (VU)

A thesis submitted in fulfillment of the requirements for the degree of Master

in

Mathematics (Biomedical track)

June 30, 2017

Declaration of Authorship

I, Judith Bouman, declare that this thesis titled, "Modeling the Appearance and Spread of Drug-Resistant Influenza" and the work presented in it are my own. I confirm that:

- Where I have consulted the published work of others, this is always clearly attributed.
- Where I have quoted from the work of others, the source is always given. With the exception of such quotations, this thesis is entirely my own work.
- I have acknowledged all main sources of help.
- Where the thesis is based on work done by myself jointly with others, I have made clear exactly what was done by others and what I have contributed myself.

Signed:

Date:

University of British Columbia
VU University Amsterdam

Abstract

Master

Modeling the Appearance and Spread of Drug-Resistant Influenza

by Judith Bouman

The impact of the annual influenza epidemic is still large; 36,000 deaths in the US each year. Elderly people are in particular vulnerable to side effects of an infection. Therefore they need to be protected against getting infected, however, vaccines are less efficient for them. Antiviral treatment can minimize the risk of side effects, but drug-resistant viruses can appear during treatment. The spread of these resistant type viruses will increase the number of deaths during an epidemic, as vulnerable patients can no longer be treated with the drug.

A mathematical model is used to describe the appearance and spread of drug-resistant viruses during an influenza outbreak in an elderly people's home. As the appearance of the resistant viruses happens within a patient under treatment, this is modeled on a within-host scale. On the contrary, the spread of resistant type influenza takes place on a between-host scale and is thus modeled as such. Resistance appears due to a combination of mutations in the viral RNA. Hence, the within-host model is stochastic and has to be modeled in that way. However Gillespie's direct stochastic simulation algorithm would be too time intensive. Therefore, a hybrid simulation method is developed. This method combines a deterministic approach with Gillespie's algorithm. The results of the within-host model are used to calculate the probability that an infected person under treatment infects a susceptible person with resistant type influenza in the between-host model.

The effect of the initial infective, different vaccinating strategies, different treatment times, different treatment rates and a different treatment-efficacy function on the epidemic in an old people's home are evaluated. The first conclusion is that the initial infective influences the probability of a major outbreak, but not the distribution of the final size of a major outbreak. Secondly, vaccinating the elderly people is more efficient in preventing the spread of resistance than vaccinating health care workers. Thirdly, treatment has to be applied as early as possible and treatment after some time is more harmful than helpful in the long term. Moreover, the treatment rate should be kept as small as possible. Finally, the treatment- efficacy function greatly influences the probability that resistance appears during treatment.

Acknowledgements

I would like to thank prof. dr. Daniel Coombs for supervising me. His advice and ideas were very useful to me. Moreover, I want to thank dr. Bob Planqué for allowing me to write my thesis at UBC. I appreciate the freedom that he gave me. Thanks to Alejandra Herrera for her comments and help. Also, thanks to prof. dr. Pauline van den Driessche for her advice on Chapter 8.

Contents

Chapter 1

Introduction

Influenza infections cause 36,000 deaths in the United States each year (McElhaney et al., 2012). Small changes in the genotype of the virus (genetic shift) are responsible for the annual recurrence of the epidemic, as they make the viruses undetectable to the immune system (Pop-Vicas and Gravenstein, 2010). Moreover, major genetic re-assortment (genetic-drift) can cause a pandemic, as happened in 2009 (Pop-Vicas and Gravenstein, 2010). The World Health Organization (WHO) declared the minimal number of deaths caused by the 2009-pandemic to be $18,449$ (Viboud and Simonsen, 2012). However, the effects could have been much worse: the expected number of deaths for a new pandemic lies between $89,000$ and $207,000$ in the United States (Meltzer, Cox, and Fukuda, 1999). The main reason for the limited number of deaths in 2009 is pre-existing immunity in 34% of the population born before 1950 (Pop-Vicas and Gravenstein, 2010). However, there is no doubt that a new pandemic will occur in the future. When this happens, prior immunity might not exist in the population.

The most effective strategy to prevent high mortality numbers is to gain immunity for part of the population by vaccinating them (Fiore et al., 2010). One major drawback of vaccines is that they only work for a limited number of virus types (Fiore et al., 2010). Therefore, each year, the WHO determines a selection of viruses that are expected in the next season. The efficiency of influenza vaccines is estimated to be 83 % when the vaccine matches the influenza strain of the season well (Darvishian et al., 2017). However, it is entirely possible that the influenza virus will evolve to a different form before the influenza epidemic occurs, making the vaccines essentially useless (Salomon and Webster, 2009). A second drawback of vaccines is that they are less effective for the elderly (Pop-Vicas and Gravenstein, 2010). The reason for this is that their immune system produces less antibodies after the administration of a vaccine, leading to a reduced immune memory compared to young, healthy individuals (Gross et al., 1995).

That elderly people have a less efficient immune system than the younger part of the population does not only influence the vaccine efficiency. An other effect is that there are differences within the course of the infection and the side effects thereof. To start with, the hospitalization and mortality rates are highest for elderly people (Lambert et al., 2012). More specifically, the elderly do not have the highest rate of infections, but they are responsible for the major part of the deaths (Lambert et al., 2012). Secondly, 3-4 months after their infection, 25 % of the people staying in an old people's home or hospital are still suffering from the loss of a major function, compared with 15.7 % of the control group (Lambert et al., 2012).

A consequence of the differences mentioned above is that the financial burden of influenza infections in elderly people compared to the rest of the population is much higher. Altogether, these are good reasons to protect the elderly from influenza infections. To do so, an addition to vaccinating is needed. Luckily, anti-viral drugs are available. These drugs cannot cure an infection, however, they shorten the infectious period and lower the probability of serious side-effects. Anti-viral drug treatment is especially useful for high risk patients in order to prevent hospitalization (Disease Control and Prevention, 2009).

Unfortunately, using anti-viral treatment has a disadvantage as well: resistance to the treatments has become more common over the past few years. Resistance can appear spontaneously in patients that undergo treatment due to mutations in the viral RNA. A patient who suffers from a resistant infection due to treatment can spread the resistant type infection further in the population. The effects are most serious for the vulnerable part of the population, for instance the elderly, as the probability of having serious side effects cannot be reduced for patients with a resistant infection.

Therefore, the focus of this thesis is to research the appearance and spread of resistant type influenza. Moreover, different strategies to prevent resistance to spread and to protect the elderly for getting infected with resistant type influenza are tested. This will be done with the use of a mathematical model. The model consists of two levels. The within-host scale describes the appearance of resistance during treatment. The spread of the infection at population level is modeled on a between-host level. The within-host model is stochastic, to properly capture the stochasticity of the mutation effect that leads to resistance. The spread between-hosts is modeled stochastically as well, as the appearance of resistance in a host is stochastic. The scale of the between-host model is that of an old people's home, where the infection has different effects on health care workers (HCW's) than on the elderly that live there.

The within-host model will first be used to evaluate the effect of different starting times of treatment on the probability that resistance appears during treatment of an elderly patient. Furthermore, the results of the within-host model are incorporated in the between-host scale. The full model (the combination of both scales) is used to answer five main questions.

First of all, what is the effect of the initial infective (elderly or HCW) on the course of the epidemic? Due to the fact that the infectious period of an elderly person is longer, the expectation is that the probability of a major outbreak is larger if the first infective is an elderly person. However, it is less clear what the effect of the initial infective is on the distribution of the final size of the major outbreaks.

Secondly, different strategies for vaccinating are tested: vaccinating the HCW's or the elderly. The goal is to discover which strategy minimizes the final size of the epidemic, while keeping the the fraction of resistant infections as small as possible. Especially, the fraction of elderly people infected with resistant type needs to be as small as possible.

Thirdly, the effect of the treatment timing is evaluated. Early treatment will greatly influence the course of the infection and prevent the infection from taking place in any significant way. On the other hand, very late treatment, when all healthy cells

are already infected with the sensitive type, will not affect the rest of the infection anymore. Between those two extremes the effect of the treatment will vary widely, however, there exists an optimal treatment time for resistance to appear. In other words, this is the treatment time that leads to the highest probability of resistance appearing. Finding this optimal treatment time for resistance will help to decide at which point treatment is useful and when it might do more harm than good.

Fourthly, different treatment rates will be applied in the model. A higher treatment rate is expected to increase the number of resistant cases in the epidemic. At the same time, it is interesting to see the trade-off between the final size and the fraction of resistant infections for different treatment rates.

Finally, a different treatment-efficiency function will be evaluated. In all previous cases the treatment is introduced at a fixed time after infection. Before this treatment time the treatment parameter in the model is zero and afterwards it is equal to the treatment efficiency. However, in reality it might be the case that the efficiency of the treatment is not a step function like this, but an increasing function. The effect of modeling the treatment as an increasing function is evaluated.

Chapter 2

Biological Background

Understanding the biological mechanisms of the replication, infection and spread of influenza is important for the modeling of the infection at the within and between-host level. Therefore, this chapter presents a description of the most important processes. In general, there are three types of influenza; A, B and C. The description is focused on type A.

2.1 Structure and Organization

A schematic representation of the spherical shaped influenza A virus is shown in Figure 2.1. The membrane of the virus contains three types of proteins; haemagglutinin (HA), neuraminidase (NA) and M2 proteins. These proteins have different functions. First of all, the two main functions of HA are to bind to the target cells and to fuse the virus membrane with the membrane of the target cell (Isin, Doruker, and Bahar, 2002). Secondly, NA makes sure that a new virus can leave the infected cell and spread through the human body (Isin, Doruker, and Bahar, 2002). Thirdly, the M2 proteins traverse the membrane and function as ion channels (Bouvier and Palese, 2008).

The core of the influenza virus is surrounded by M1 proteins and contains nuclear export protein (NEP) and viral ribonucleoprotein complex (vRNP) (Bouvier and Palese, 2008). vRNP consists of viral RNA coated with nuclear proteins and RNA polymerase (Bouvier and Palese, 2008). The viral RNA is divided in eight segments, of which four code for only one protein (Bouvier and Palese, 2008).

Influenza viruses do not have proofreading proteins in their core. Therefore, the mutation rate of the virus RNA is high compared to organisms that do have proofreading proteins. Furthermore, the rate of multiplication of RNA viruses is high. Together this results in high genetic variability between influenza types (Holland et al., 1982).

The division of the genome in multiple segments explains how genetic shifts take place. As four out of eight segments only code for one protein, such a segment could be replaced with a segment coding for the same protein from a different type of influenza virus. However, this segment can be different and can have different features. An event like this usually happens when an organism is infected with two different types of influenza at the same time.

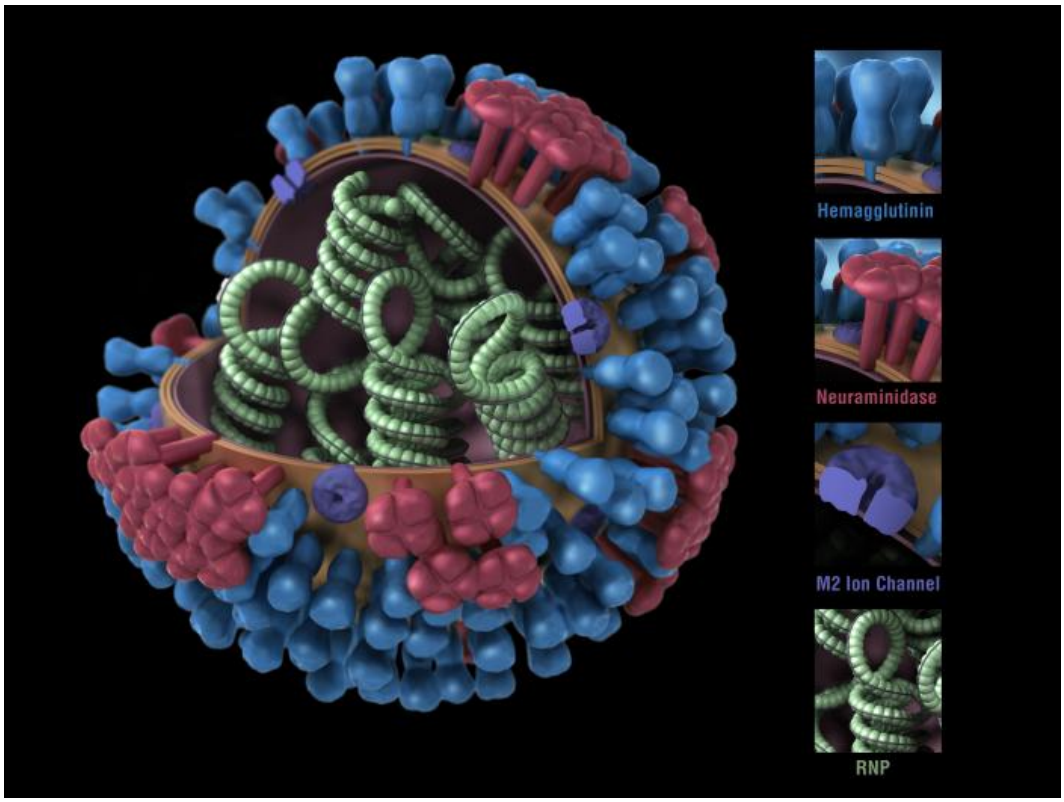

FIGURE 2.1: Schematic representation of a influenza A virus (Jordan, 2014).

2.2 Mechanism of Infection

An influenza infection has various ways to spread between organisms. The first option is by direct contact with an infective, the second by contact with a contaminated object and the third one by breathing in aerosols containing viruses (Racaniello, 2009). As soon as a virus enters the body of the susceptible host and comes into contact with a host cell, HA binds to a protein on the membrane of the host cell. Part of the HA protein penetrates the host membrane and brings the virus and host cell membranes together. Next, the ion channels open and the vRNAs can freely move to the host cell.

In order to replicate the vRNA, they must enter the nucleus (Samji, 2009). Once the vRNA is inside the nucleus of the host cell, the virus hijacks the cells reproduction machinery to replicate its RNA (Samji, 2009). The new RNAs move back to the cytoplasm of the cell and use the cell's translation mechanism to synthesize the proteins coded by the RNA. M2 proteins make sure that the right RNA molecules and proteins come together. Moreover, M2 establishes a new membrane for the virus using the hosts cell membrane. The M1 proteins have an important function in closing the membrane. Before the virus can leave the host cell, it must cleave off receptor proteins from the membrane. This last step is crucial as new viruses can not be formed without it (Samji, 2009). These steps of replication are shown in Figure 2.2.

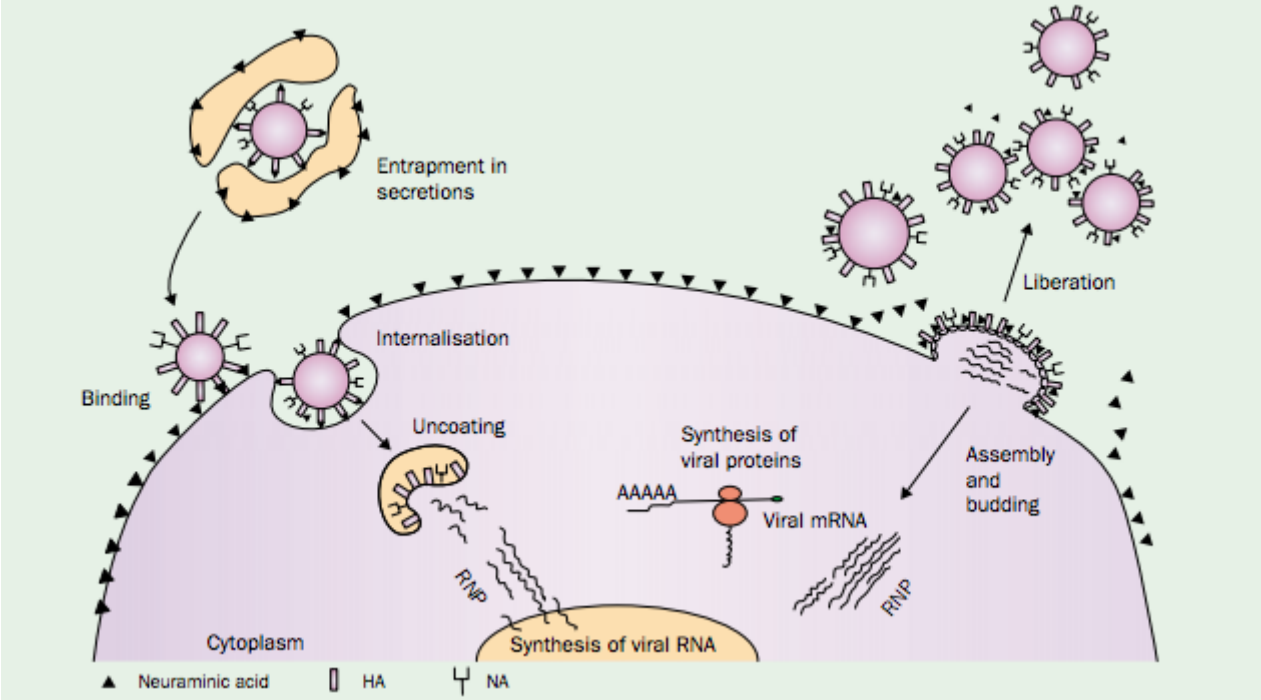

FIGURE 2.2: Overview of Influenza life cycle (Gubareva, Kaiser, and Hayden, 2000).

2.3 Immune Response and Vaccines

An immune response is induced when antigens from the virus are fragmented by macrophages. Some of these fragments are presented by major histocompatibility complex (MHC) molecules on their cell membrane. These complexes are recognized by T-cells, which stimulate B-cells to produce antibodies. The T-cells respond to the MHC molecules beaming antigenic fragments only. Therefore, it does not make a difference if the fragments are derived from actual viruses or from vaccines (Medicine, 1997).

Antibodies to NA and HA proteins are most important in obtaining resistance to the infection, whereas antibodies to M and NP proteins play a crucial role in the clearance of the infection and recovery of the patient (Cox, Brokstad, and Ogra, 2004). The immune response protects against reinfection until the virus has evolved such that the antibodies cannot recognize the proteins anymore. This process usually takes several years (Cox, Brokstad, and Ogra, 2004). Genetic-drift causing a pandemic is estimated to happen three times every 100 years (Treanor, 2004).

Vaccines contain impaired viruses to trigger the immune response without causing an infection. The estimates of the efficiency of vaccines to create immunity to influenza vary. Darvishian et al. (2017) found that an influenza vaccine has an efficiency of 83 % when the vaccine matches the circulating viruses well. On the contrary, poorly matched vaccines may be only 20 % effective. In general, the vaccine efficiency for influenza lies between 60 and 90 % for well matched vaccines (Cox, Brokstad, and Ogra, 2004). A pooled estimate for the efficiency of preventing respiratory illness with vaccines in elderly persons is 56 % (Gross et al., 1995).

2.4 Treatment

Multiple types of influenza treatment are on the market. The focus of the thesis is on *Oseltamivir*, because resistance to this drug occurred during the pandemic of 2009 for the first time. *Oseltamivir* belongs to the group of NA-inhibitors (Moscona, 2005). Therefore, it functions by prohibiting the last step of production of new viruses. Thus, the treatment prevents the production of new viruses, but does not kill the ones that already exist. The result thereof is that treatment with this drug is only useful before the peak of virus production during the infection (Moscona, 2005).

2.5 Appearance of Resistance

As mentioned before, the mutation rate of RNA viruses is relative high. The first effect thereof is already discussed above; the immunity to an infection is lost after a curtain amount of time. The second effect of the high mutation rate is that treatment resistant types of the virus can appear during the course of an infection. The probability of a mutation estimated to be 7×10^{-5} by Drake (1993) and 2×10^{-6} by Nobusawa and Sato (2006). However, one mutation is not sufficient to obtain resistance. The process of obtaining resistance is a multi-step process (Gubareva et al., 1996). In vitro studies by Gubareva et al. (1996) showed that there are two main steps in the process. The first is a reduction of the dependence of the virus on the NA activity, by changes in the HA protein. The second step includes changes in the NA protein itself.

The mutation rate of one point-mutation is thus not equal to the overall mutation rate to obtain *Oseltamivir*-resistance. As multiple mutations are needed, the probability to find them together is expected to be smaller than for a single mutation. Multiplying the number of point mutations to get the resistance is not a solution, as some mutations can be linked together. However, the mutation rate to obtain this type of resistance is not known from biological experiments. Therefore, it has to be estimated.

Obtaining *Oseltamivir*-resistance is at the cost of the fitness of the virus (Hurt et al., 2010). Therefore, resistant-viruses that appear when there is no treatment cannot compete with the sensitive type. Resistance will therefore not appear without applying treatment. Under treatment, the fitness of the resistant type viruses is much higher than for the sensitive type and they will spread within the host (Xiao, Brauer, and Moghadas, 2016). As a result, this host can spread the resistant type influenza to others.

Chapter 3

Mathematical Background

In this chapter the mathematical techniques that are used in the rest of the thesis are briefly discussed.

3.1 Gillespie Algorithm

Consider a process involving M species. Let the amount of species m be given by x_m. The dynamics of these species are usually described by a set of M coupled ordinary differential equations. Solving these equations results in a deterministic solution for the system. However, this solution is not adequate when the process is, for instance, subject to a stochastic event (Gillespie, 1977). In later chapters it will become clear that this is the case for the models that are studied in this thesis. Therefore, this section will describe an algorithm to simulate trajectories of a stochastic process.

Gillespie (1977) designed such an algorithm, where each single result of the algorithm is a sample from the probability mass function that is the solution of the master equation. The master equation describes the time derivative of the probability of the system to be in a specific state. When executing the Gillespie algorithm there is no need to explicitly write this master equation. The algorithm is based on the reactions that make up the process. The reactions can be found by examination of the M ODEs.

The basic idea behind the algorithm is that for each new step in the process two random numbers are chosen. One is the time interval before the next reaction takes place and the second one indicates which reaction will occur at this new time point. The algorithm is structured as shown in Figure 3.1.

To explain the algorithm, a simple example will be used. Four different species (S_1, S_2, S_3 and S_4) are considered. Suppose their dynamics are described by;

$$\frac{dS_1}{dt} = -a_1 S_1 S_2, \tag{3.1}$$

$$\frac{dS_2}{dt} = -a_1 S_1 S_2, \tag{3.2}$$

$$\frac{dS_3}{dt} = a_1 S_1 S_2 - a_2 S_3, \tag{3.3}$$

$$\frac{dS_4}{dt} = a_2 S_3. \tag{3.4}$$

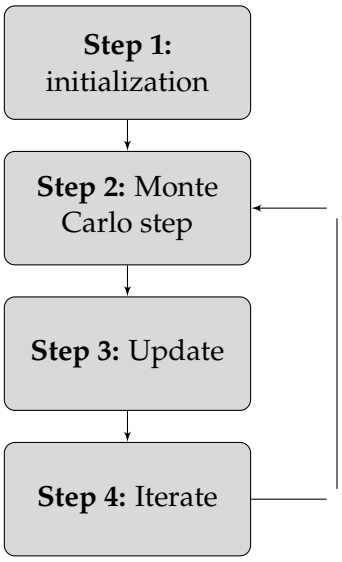

FIGURE 3.1: Schematic representation of Gillespie algorithm (Gillespie, 1977).

These equations indicate that species S_1 and S_2 react together to produce S_3 with rate a_1 and S_3 becomes S_4 with rate a_2. Therefore, the reactions corresponding to this ODE system are;

$$S_1 + S_2 \rightarrow S_3, \tag{3.5}$$

$$S_3 \rightarrow S_4. \tag{3.6}$$

The first step of the algorithm is to initialize the amount of each species, the propensity of each reaction and the generator of the next time step. The propensities are calculated for each reaction by multiplying the reaction constant with the amount of the species on the left side of the reaction. For the example case, the propensities would be $p_1 = a_1 x_1 x_2$ and $p_2 = a_2 x_3$ for respectively reaction 1 and 2. The total propensity (p_{tot}) is given by the sum of the propensities of each species. The generator of the next time interval is an exponential distribution with mean p_{tot}.

The second step of the algorithm is to pick the time interval (δt) from the distribution described above. Moreover, the reaction that will take place at the next time step is chosen. The probability to pick reaction i is given by $\frac{p_i}{p_{tot}}$ for all reactions in the system. A reaction will be chosen corresponding to these probabilities.

After performing the chosen reaction, the propensities are updated during step 3 and the time is updated by δt. Step 4 is to iterate the past two steps for as many times as needed.

3.2 Statistical tests

To test the difference between observations of two binomial processes, for instance number of major outbreaks of two different strategies, the following test statistic is used;

$$T = \frac{\hat{p_1} - \hat{p_2}}{\sqrt{p^\star(1-p^\star)(\frac{1}{n_1} + \frac{1}{n_2})}}, \tag{3.7}$$

where $p^\star = \frac{x_1+x_2}{n_1+n_2}$, x_1 and x_2 are the number of successes in respectively the first and the second case, p_1 and p_2 are the observed probability for respectively the first and the second case and n_1 and n_2 are the number of experiments for both cases. For a high enough number of observations, this test statistic follows a normal distribution. The reported p-values are all for the two-sided variant of the test. This test will be referred to as the *binomial test* for the rest of the thesis.

The difference between two distributions is tested with a Mann-Whitney U test. This is a non-parametric test to test whether two sets of observations are drawn from the same distribution.

Chapter 4

Within-host Model

This chapter describes a model of the within-host dynamics of an influenza infection. Furthermore, it explains how the model is simulated, using a hybrid combination of a direct simulation method (Gillespie's algorithm) and a deterministic approach.

4.1 Description of the Model

The within-host model is based on Handel, Longini Jr, and Antia, 2007. A schematic version of this model is shown in figure 4.1. Here, χ represents the healthy cells in the respiratory tract of the host. If one of the healthy cells gets infected with sensitive virus it will go the L_s stage (latent infection), where the cell does not produce any new viruses yet. From there, the cell will evolve to the next stage; Y_s, in which it does produce new sensitive viruses (V_s). After some time, the cell will leave this state by dying. It is assumed that turnover of healthy cells is slow on the timescale of infection and therefore birth and death of uninfected cells (χ) is neglected.

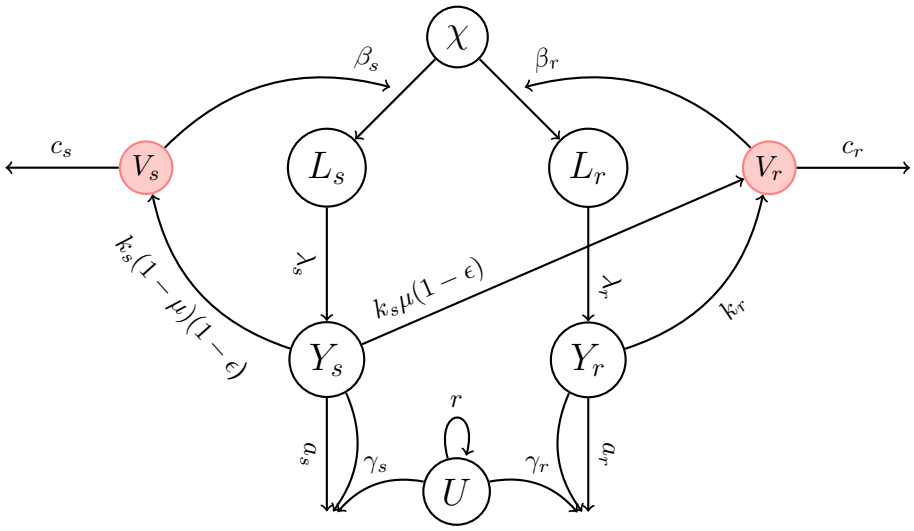

FIGURE 4.1: Overview of the within-host model including categories for free viruses.

With probability μ, a mutation will occur during the transcription of new viruses by a cell in Y_s, this mutation causes the viruses to be resistant to anti-viral treatment.

These resistant viruses are capable of infecting healthy cells as well. Cells infected by resistant type virus will go to the L_r state, from where they will move to Y_r. Here, they produce new viruses, which are all resistant to treatment (V_r); back mutations to sensitive type are not possible.

The infection will induce an immune response in the host, as explained in Section 2.3. The effects thereof are broad. Various ways exist to include this in the model. Here, a very simple approach is chosen: the immune response is modeled as a single dynamic variable U. This variable determines the rate of killing of infected cells. It is assumed that the dynamics of U are independent of the rest of the model. The main reason for including an immune response to the model is to be able to differentiate between healthy, young hosts and elderly hosts. The most important difference between these two groups is the duration of the infection, which is longer for the elderly. The proposed simple way to model the immune response makes it possible to adapt the duration of the infection with one parameter and is therefore very suitable for the goal in mind.

The ODE version of the model described above is:

$$\dot{\chi} = -\beta_s \chi V_s - \beta_r \chi V_r, \tag{4.1a}$$
$$\dot{L_s} = \beta_s \chi V_s - \lambda_s L_s, \tag{4.1b}$$
$$\dot{L_r} = \beta_r \chi V_r - \lambda_r L_r, \tag{4.1c}$$
$$\dot{Y_s} = \lambda_s L_s - a_s Y_s - \gamma_s U Y_s, \tag{4.1d}$$
$$\dot{Y_r} = \lambda_r L_r - a_r Y_r - \gamma_r U Y_r, \tag{4.1e}$$
$$\dot{V_s} = -\beta_s \chi V_s + k_s(1-\epsilon)(1-\mu) Y_s - c_s V_s, \tag{4.1f}$$
$$\dot{V_r} = -\beta_r \chi V_r + k_r Y_r + \mu k_s (1-\epsilon) Y_s - c_r V_r, \tag{4.1g}$$
$$\dot{U} = rU(Q-U). \tag{4.1h}$$

The parameters of the model, for respectively the sensitive and the resistant strain, are; the rate of transition from the latent state to the infectious state, λ_s and λ_r; the death rate of infected cells, a_s and a_r; the infectivities, β_s and β_r; the virus reproduction rates, k_s and k_r; the rate with which infected cells are killed by the immune response, γ_s and γ_r and the expansion of the immune response, r. Finally, Q indicates the maximal number of immune cells U in the model.

The effect of treatment is indicated by ϵ, which represents the efficiency of the treatment. The absence of treatment can be modeled by setting ϵ to zero and treatment by $\epsilon \geq 0$ during a specific period of the infection. As explained in Section 2.4, treatment affects the production of new viruses by a cell infected with sensitive type. Furthermore, it only influences the sensitive type, as the resistant cells are assumed to have evolved in such a way that they do not response to the treatment anymore.

Simplified Version of Within-host Model

The level of free viruses can become very large in Model 4.1 and consequently a direct simulation of the model with Gillespie's algorithm will be very time intensive.

This is because the production of a single virus is one reaction and each reaction takes one step of in the algorithm. For this reason, the model is simplified to the one represented in Figure 4.2.

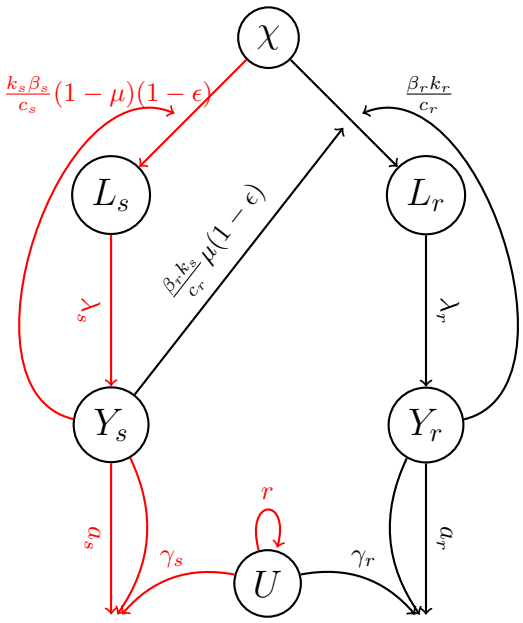

FIGURE 4.2: Overview of the within-host model without free virions.

In order to obtain the simplified model, some assumptions are necessary. First of all, one infected cell produces relative many new viruses. On the other hand, the stability of viruses is low compared with the stability of infected cells. Hence, c_s and c_r are large with respect to a_s and a_r. As a result of these two observation it can be concluded that the dynamics of the free viruses are much faster than the dynamics of the cells. Therefore, it is assumed that the free viruses are in a quasi steady state $\Rightarrow \dot{V}_s = 0 = \dot{V}_r$.

The second assumption is that the loss of free viruses due to infection of healthy cells is negligible, as there are many more viruses than infected cells $\Rightarrow \beta_s \chi V_s = 0 = \beta_r \chi V_r$. The quasi steady state levels of V_s and V_r can now be found by setting Equation 4.1g and 4.1h to zero and solving using the second assumption. The result is;

$$V_s^{q.s.} \approx \frac{k_s}{c_s}(1-\epsilon)(1-\mu)Y_s \text{ and } V_r^{q.s.} \approx \frac{k_r Y_r + \mu k_s (1-\epsilon) Y_s}{c_r}. \tag{4.2}$$

System 4.1 can then be simplified to:

$$
\begin{aligned}
\dot{\chi} &= -\beta_s \chi \frac{k_s}{c_s}(1-\epsilon)(1-\mu)Y_s - \beta_r \chi \frac{k_r Y_r + \mu k_s (1-\epsilon) Y_s}{c_r}, \\
\dot{L_s} &= \beta_s \chi \frac{k_s}{c_s}(1-\epsilon)(1-\mu)Y_s - \lambda_s L_s, \\
\dot{L_r} &= \beta_r \chi \frac{k_r Y_r + \mu k_s (1-\epsilon) Y_s}{c_r} - \lambda_r L_r, \\
\dot{Y_s} &= \lambda_s L_s - a_s Y_s - \gamma_s U Y_s, \\
\dot{Y_r} &= \lambda_r L_r - a_r Y_r - \gamma_r U Y_r, \\
\dot{U} &= rU(Q-U).
\end{aligned} \tag{4.3}
$$

4.2 Choice of Parameters

The parameters of the model are chosen such that the model obeys the following rules of thumb:

- the duration of the disease is 5 days in healthy individuals (Pop-Vicas and Gravenstein, 2010),
- elderly individuals have a disease time of 7 days (Pop-Vicas and Gravenstein, 2010),
- the peak in the infection takes place after 2/3 days in healthy individuals (Hadjichrysanthou et al., 2016).

Furthermore, the mutation rate is tuned such that the number of times that resistant type viruses appear corresponds with observations. Several estimates of the prevalence of resistant type influenza can be found in literature; for instance 1.4 % in Mai-Phuong et al., 2013 and 1.7 % in Meijer et al., 2011. In this last reference 1100 patients were followed and 17 developed a resistant type influenza infection while they underwent Oseltamivir treatment. The resistant cases were all kept in successful isolation and therefore no secondary resistant infections were observed. To observe similar percentages of the appearance of resistance in the within-host model, the mutation rate is set to 10^{-8}. However, these prevalences are also dependent on the treatment time. This is examined in Section 7.1.1.

Paradis et al., 2015 performed experiments in ferrets with the 2009 pandemic H1N1 strain to find values for the parameters in both the sensitive and resistant strain. However, direct use of their parameters in the model does not give the desired results. This is not surprising, as the reproducibility of these kinds of experiments is usually low and the used models do not correspond one-to-one with each other. The main difference is that the model of Paradis et al., 2015 does not include an immune response. However, the relative difference between the values measured for sensitive and resistant strain are useful for the model. They are measured under the same circumstances in competition experiments and are therefore more trustworthy than the absolute values of the separate parameters.

Ultimately, the parameters used for the model are shown in Table 4.1. The parameters for the sensitive strain are chosen so that the model obeys the rules of thumb described above in a healthy individual. The immune response is altered such that

the infection will take two extra days in elderly patients. Furthermore, the parameters for the resistant strain are chosen based on the relative difference between the two strains found by Paradis et al., 2015.

The initial number of healthy cells is set to 4×10^8, which is the number of cells in the human air trajectory as calculated by Baccam et al. (2006). Each infection starts with 100 infected cells in the latent state of either the sensitive or the resistant type. The initial condition for the number of cells in the immune system is responsible for the difference in the duration of the infection. For healthy persons the initial number of immune cells is 100 and for elderly only 20. All other species start with an initial condition of zero. Examples of results of the model using the reported parameters and initial conditions are shown in Figure **??** until **??**.

TABLE 4.1: Parameters of within-host model.

Parameter	Value for Sensitive Strain	Value for Resistant Strain
β	3.1×10^{-10} $[V_s]^{-1}h^{-1}$	2.4×10^{-10} $[V_r]^{-1}h^{-1}$
k	6 $[V_s][Y_s]^{-1}h^{-1}$	17.5 $[V_r][Y_r]^{-1}h^{-1}$
c	1.116 h^{-1}	1.116 h^{-1}
λ	0.050 h^{-1}	0.033 h^{-1}
a	0.054 h^{-1}	0.136 h^{-1}
γ	1×10^{-5} $[U]^{-1}h^{-1}$	1×10^{-5} $[U]^{-1}h^{-1}$
r	25×10^{-7} h^{-1}	25×10^{-7} h^{-1}
Q	2000	2000

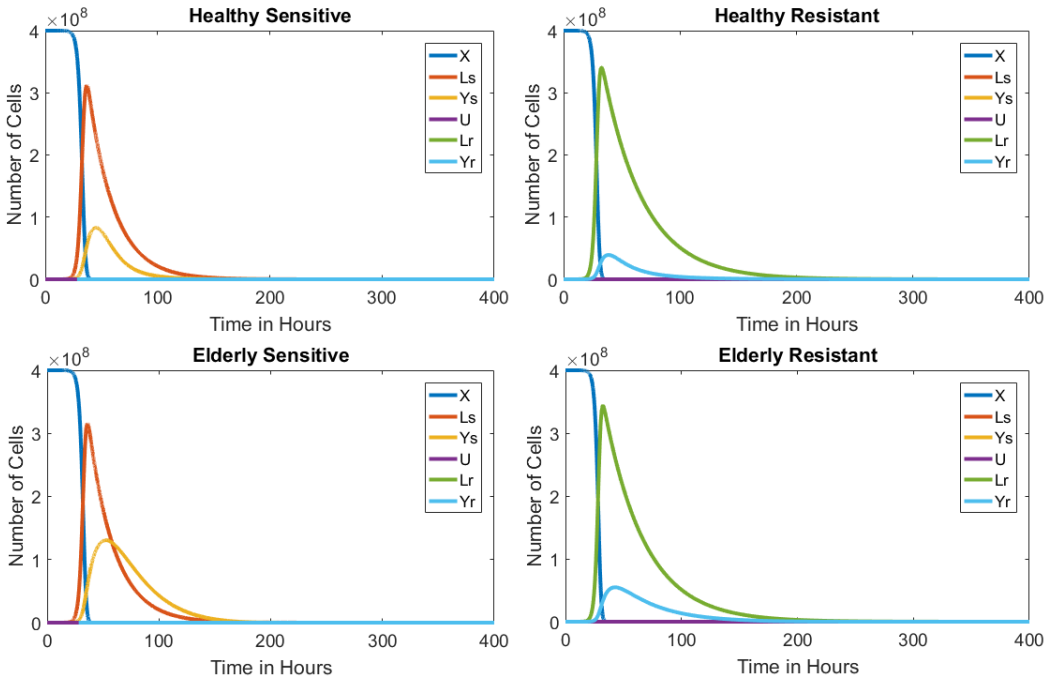

FIGURE 4.3: Example of the output of a simulation of the within-host model for each type of infection.

4.3 Method of Modeling

Solving the within-host model with a standard ODE solver in *Matlab* does not give the desired results. The reason for this is that the probability to mutate from sensitive to resistant type virus is very small. It will appear as a low but steady flow in the deterministic solution. However, as will be shown later in this chapter, the timing of the mutations is crucial for the appearance of resistance. Therefore, a stochastic method is more suitable for the model, as it allows for mutations at variable time points.

4.3.1 Hybrid Simulation Method

To simulate the within-host model stochastically, the algorithm of Gillespie (1977) could be used. As explained in Section 3.1 the reactions of the model are needed in addition to the ODE description. These are summarized and numbered in table 4.2.

The initial number of healthy cells is 4×10^8 (Baccam et al., 2006). With this initial condition the number of reactions is of the order of magnitude of 10^9 per hour during the first part of the infection. Hence, the simulation time of a Gillespie simulation of the model will be impractically high, despite the simplification that is already made in Section 4.1. However, the major part of these reactions will be reaction 1, 3, 5, 7 or 8 from Table 4.2, which we will refer to as the fast reactions. These fast reactions are indicated in red in Figure 4.2 and have great influence on the behavioral of χ, L_s and Y_s; the fast species. In contrast, reaction 2, 4, 6, 9 and 10 (the slow reactions), fire much less frequently and mainly influence the level of Y_r and L_r (the slow species). They will not have significant effect on the fast reactions as long as the number of cells in Y_r and L_r are still relatively small.

TABLE 4.2: Reactions and their rates of the within-host model.

	Reaction	Reaction Rate
1	$\chi + Y_s \rightarrow L_s + Y_s$	$\frac{k_s \beta_s}{c_s}(1-\mu)(1-\epsilon)$
2	$\chi + Y_r \rightarrow L_r + Y_r$	$\frac{\beta_r k_r}{c_r}$
3	$L_s \rightarrow Y_s$	λ_s
4	$L_r \rightarrow Y_r$	λ_r
5	$Y_s \rightarrow null$	a_s
6	$Y_r \rightarrow null$	a_r
7	$Q \rightarrow U$	r
8	$Y_s + U \rightarrow null$	γ_s
9	$Y_r + U \rightarrow null$	γ_r
10	$\chi + Y_s \rightarrow L_r + Y_s$	$\frac{k_s \beta_s}{c_s}\mu(1-\epsilon)$

In conclusion, the simulation of the model can be made faster by using a deterministic approach whenever possible: for the fast part of the model and for the complete model if the number of cells in the slow category is large enough. The rest of this section describes the algorithm that is constructed to simulate the model in this way, which is referred to as the **hybrid simulation method**.

The idea behind the **hybrid simulation method** is to simulate the number of mutation events (reaction 10) and their timing based on the deterministic solution of the fast part of the model. Reaction 10 is the link between the fast and the slow part of the model. If the activity of this reaction is known, then the slow part can be simulated with Gillespie's algorithm. The advantage is there is no need to simulate the fast reactions in the Gillespie algorithm. Therefore the number of reactions is much lower and the algorithm is faster. When the number of cells in Y_r and/or L_r reach the level at which they start to influence the dynamics of χ (the switching level) the full model is solved deterministically for the remaining part of the infection. Further mutation events after this point are dealt with deterministically.

The **first step** of the hybrid simulation method is to evaluate the fast part (reaction 1, 3, 5 and 8) deterministically. This results in the dynamics of χ, Y_s, L_s and U during the time of the infection if there is no successful mutation. Each time a cell in Y_s infects a healthy cell there is a probability of μ that this results in a resistant type infection. During **step 2** of the algorithm, the deterministic solution of step 1 is used to measure the number of times a healthy cell gets infected, which will be referred to as N.

In the situation without treatment, all healthy cells will get infected and N will thus equal the initial number of cells; 4×10^8. If treatment is applied to the patient, N can be smaller than the total number of initial healthy cells. As mentioned before, the probability to get a resistantly infected cell is μ for each reaction that takes place. Consequently, the number of mutation events follows a binomial distribution with N independent experiments and probability of success equal to μ. In the **third step** of the algorithm the number of mutation events is chosen from this binomial distribution.

Now the number of mutation events is known, the **4th step** is to estimate the time at which each event takes place. The probability that a mutation event occurs at time t is proportional to the number of times that reaction 10 takes place at time t. This quantity is proportional to the propensity of reaction 10. Therefore, the time of each mutation event is drawn from the distribution that is obtained by multiplying the amount of cells in χ with the amount of cells in Y_s followed by a normalization. This distribution for the situation without treatment is shown in Figure 4.4.

After completing the first 4 steps, the number and timing of mutation events is known. Therefore, the link between the fast and slow part in the model, reaction 10, is eliminated. The given mutation events will be used to simulate the slow part of the model with a direct simulation via the Gillespie algorithm. The starting time for the Gillespie algorithm will be the moment of the first mutation event. For the first step of Gillespie's algorithm the propensity of each reactions in the slow part (2, 4, 6 and 9), is calculated as described in Section 3.1. The propensity of reaction 2 is dependent on the number of healthy cells. Hence, the deterministic solution of the fast part is used to find the propensity of reaction 2.

As with a normal Gillespie algorithm, the next time interval is drawn from an exponential distribution with mean p_{tot}. However, when the next time point is later than

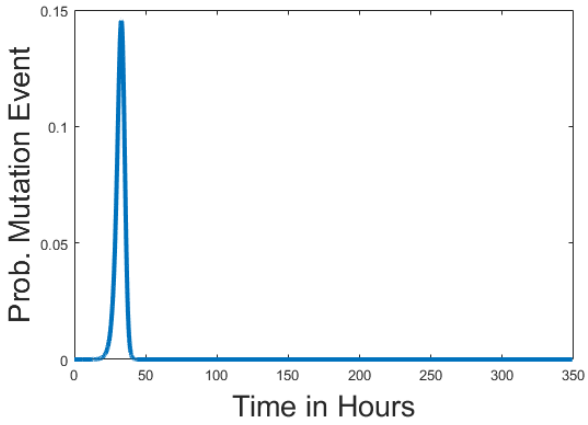

FIGURE 4.4: Probability density of mutation events during an infection.

the next mutation event, the next time point will be the next mutation event. At this time point the propensities will be updated and a new time interval is drawn from the updated distribution. These steps are iterated for as long as the infection period takes, or until the sum of the number of cells in L_r and Y_r exceeds the switching level.

If the sum of the number of cells in L_r and Y_r exceeds the switching level, then the rest of the simulation is done with a deterministic approach for the full model and the fast part is then updated as well. The output of the algorithm is the full dynamics of both the fast and the slow species over the duration of the infection.

4.3.2 Pitfalls of the Hybrid Simulation Model

The number of reactions is very high when the full within-host model is simulated with a Gillespie algorithm. This has a negative influence on the time that the algorithm takes. However, it also results in small time steps between the reactions that take place. Therefore, the propensities of the reactions are updated very regularly. The hybrid simulation model has far fewer reactions and the number of time steps is thus lower as well. Therefore, this method can underestimate the number of times a resistantly infected cell infects a healthy cell compared to a full Gillespie of the model. In both cases the propensity of reaction 2 is going down, however the decrease will be less per time step with the full Gillespie algorithm, as the steps are smaller (more reactions) than for the hybrid simulation method.

The bias is reduced by adding an empty reaction in the Gillespie algorithm of the slow part with a relative high propensity in the hybrid simulation method, such that the time steps of the simulation are decreased. The reaction rate of this empty reaction influences the results of the algorithm. Examples of different rates are shown in Section 4.4. It is important that the rate is faster than the rates of the slow reaction and that it is of the same order of the propensities in the full Gillespie version. The reason is that if p_{tot} is similar for both models, then the time steps will be of similar size as well. The propensities of the reduced model used for the comparison of the hybrid simulation method (Section 4.4) are of the same order as the propensities in the full scale model, because although the initial conditions are different, this is compensated by the different parameters. Hence, the reaction rate that gave good

results in on the reduced scale is used for the full scale as well. This rate is $90h^{-1}$.

Moreover, the switching level at which the Gillespie algorithm is interchanged for a deterministic approach has to be determined. This is chosen based on the results of Diekmann and Britton, 2012. They state that the epidemic behaves like a stochastic branching process until the square root of the total number of cells in the system is infected, after that it can be described with a deterministic solution. In this case that would mean that a deterministic approach is justified starting from 10000 cells. However, the potential influence of the resistantly infected cells on the fast part of the model has to be taken into account as well. In theory, even a very limited amount of cells influences the infection of healthy cells with either type. Hence, a threshold of switching of 10000 cells underestimates the influence of the slow part on the fast part. Therefore, the switch is already made if the sum of L_r and Y_r exceeds 1000 cells. Examples of the effect of the switching level are included in Section 4.4 for the reduced scale model.

In theory, if the treatment efficiency is not equal to one, it is possible that a mutation event takes place after the start of the treatment. However, in the hybrid simulation method this possibility is not encoded. The reason is that if a mutation can take place at any time after the treatment has started, the probability that a mutation takes place goes to one if time goes to infinity. As with a treatment efficiency that is smaller than one healthy cells keep getting infected with a low rate. That would implicate that each simulation would result in a resistant infection some time after the infection. However, in reality the immune system makes sure that an infection is not possible anymore after some time. Therefore, mutations are no longer possible after the treatment has started. Resistance can thus only occur if it appeared before the start of treatment. The comparison of the method with a full Gillespie approach in the next section shows that this assumption does not have a big impact on the results.

The algorithm described above is programmed in Matlab and the code can be found in Appendix B.1.

4.4 Comparison with Full Gillespie Algorithm

In this section, the results of the within-host model simulated with the hybrid method are compared with the results of using a full stochastic evaluation. The full stochastic variant is a standard Gillespie algorithm. The interest here is whether the hybrid method gives similar results as the full Gillespie. Therefore, the used parameters and starting conditions are chosen such that both methods can be executed within a small time window. The parameters chosen to do so are shown in Table 4.3. In order to compare the results with a limited amount of simulations, the expected number resistant cells appearing has to be high. Hence, the mutation rate μ is set to 10^{-3} for the results of this section.

Before comparing the hybrid simulation method with a full Gillespie approach, the full Gillespie is first compared to the deterministic solution of the system. In Figure A.1 the mean of 300 Gillespie simulations is compared to the deterministic solution

TABLE 4.3: Parameters for simplified within-host model for comparison between full Gillespie algorithm and hybrid simulation method.

Parameter	Value for Sensitive Strain	Value for Resistant Strain
β	$0.5 * 10^{-5} \quad [V_s]^{-1}h^{-1}$	$0.4 * 10^{-5} \quad [V_r]^{-1}h^{-1}$
k	$1 \quad [V_s][Y_s]^{-1}h^{-1}$	$1 \quad [V_r][Y_r]^{-1}h^{-1}$
c	$1 \quad h^{-1}$	$1 \quad h^{-1}$
λ	$0.15 \quad h^{-1}$	$0.16 \quad h^{-1}$
a	$0.05 \quad h^{-1}$	$0.05 \quad h^{-1}$
γ	$0.0003 \quad [U]^{-1}h^{-1}$	$0.0003 \quad [U]^{-1}h^{-1}$
r	$0.00004 \quad h^{-1}$	$0.00004 \quad h^{-1}$
Q	2000	2000

for the model without treatment. This is done for the number of cells that are infected with resistant type influenza.

For five different treatment times 100 simulations are performed with both methods. In order to compare the results thereof, the means of the simulations are shown for each treatment time in Figure 4.5 until 4.10. Dashed lines indicate the standard deviation in the simulations.

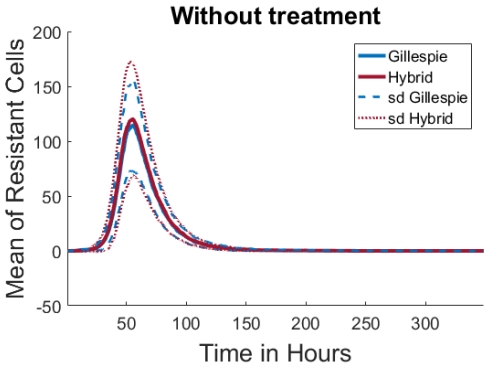

FIGURE 4.5: The means of the number of resistant cells during an infection without treatment of 100 simulations with both techniques are shown. Dotted lines indicate the 1 standard deviation from the mean.

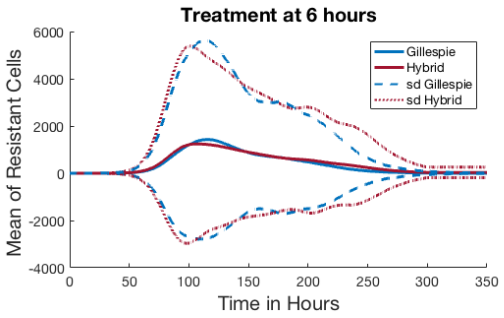

FIGURE 4.6: The means of the number of resistant cells during an infection with treatment at 6 hours after infection of 100 simulations with both techniques are shown. Dotted lines indicate the 1 standard deviation from the mean.

The mean and standard deviations of the simulations are seen to be similar for the situation where no treatment is applied. The variance is large for treatment at 6 hours after the start of the infection (see Figure 4.6). In most cases the resistant does not come up for treatment at 6 hours, as the probability that a resistant has appeared before the start of the treatment is very small. Therefore, most realizations of the model have constantly zero resistantly infected cells for this case. However, if a resistant virus appears it will have a very high probability (almost one, see results of full scale model in Section 7.1.1) to spread widely and infect almost all healthy cells with resistant type. Thus, the variance in the number of resistantly infected cells, for treatment at 6 hours is large. This is illustrated in Figure 4.7, where only 15 simulations out of 100 of the full Gillespie method and 11 simulations out of 100 of the hybrid method result in the appearance of resistance. All other simulations are very

close to zero over the duration of the infection. As a result, the mean is close to zero compared to the variance, leading to negative values if the standard deviation is subtracted from the mean. To a lesser extent, the same reasoning explains the variance in the case of treatment at 18 hours after the infection.

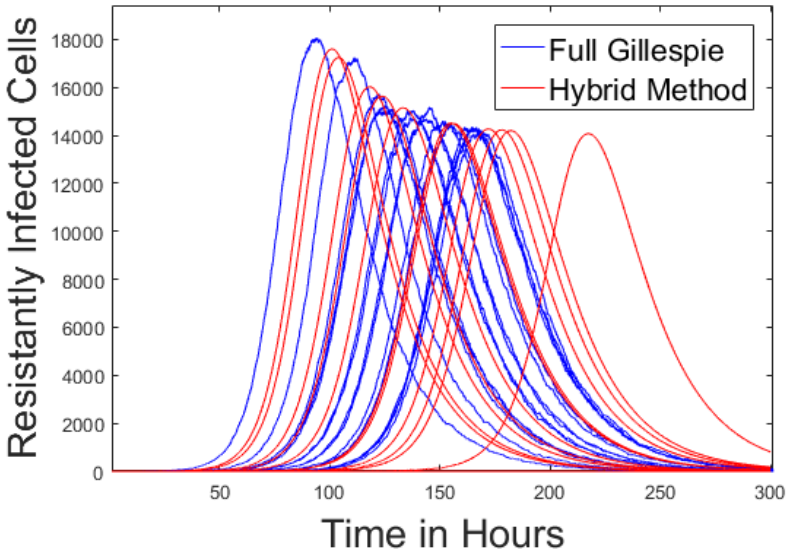

FIGURE 4.7: The number of resistant cell of 100 simulations of the within-host model for treatment at 6 hours after infection.

Figure 4.9 shows that the means and standard deviations for both methods are very similar if treatment is applied at 30 hours after infection.

The standard deviation of the full Gillespie algorithm is significantly larger than the standard deviation in the hybrid simulation method in Figure 4.10. Treatment at 42 hours is relatively late, as most healthy cell are already infected with sensitive type or death. The cells infected with resistant type that are alive at 42 hours have less opportunities for growth compared to earlier treatment. In the hybrid simulation method, the number of healthy cells available at the start of treatment will always be the same, at it is the result of a deterministic solution. However, in the full Gillespie variant the level of healthy cells at 42 hours varies. Therefore, the variance in the full Gillespie algorithm is larger than for the for the hybrid simulation method at 42 hours.

The before-mentioned difference in variance is not observed for the other treatment times. For treatment at 6, 18 and 30 hours the reason thereof is that the variance in the level of the healthy cells is lower, as the level is still almost the full initial number. For the situation without treatment and treatment at 54 hours, the variance is only coming from the number of mutation events that take place, which is the same for both techniques. The resistant cells have no opportunity for growth so the number of healthy cells does not influence the dynamics of the resistant cells.

The results of treatment at 54 hours after infection are equivalent to the results of the simulations without treatment. This illustrates that treatment has no influence on

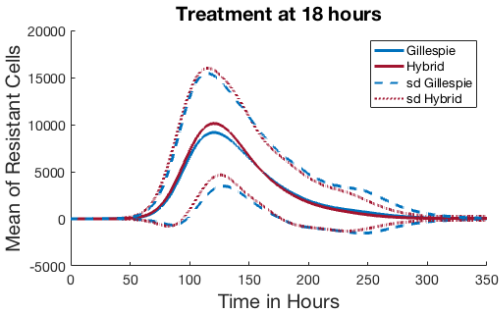

FIGURE 4.8: The means of the number of resistant cells during an infection with treatment at 18 hours after infection of 100 simulations with both techniques are shown. Dotted lines indicate the 1 standard deviation from the mean.

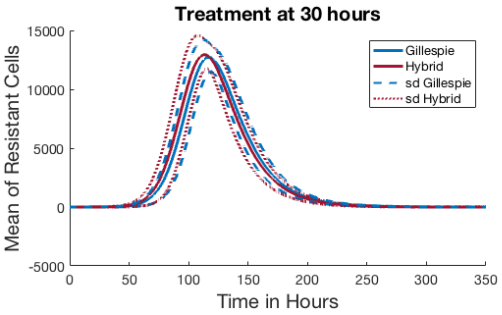

FIGURE 4.9: The means of the number of resistant cells during an infection with treatment at 30 hours after infection of 100 simulations with both techniques are shown. Dotted lines indicate the 1 standard deviation from the mean.

the simulation when it is applied after 54 hours.

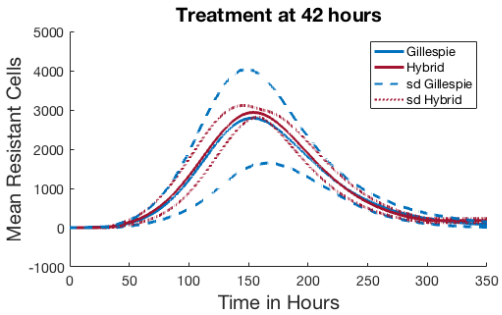

FIGURE 4.10: The means of the number of resistant cells during an infection with treatment at 42 hours after infection of 100 simulations with both techniques are shown. Dotted lines indicate the 1 standard deviation from the mean.

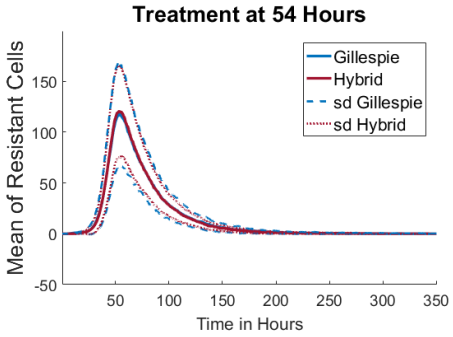

FIGURE 4.11: The means of the number of resistant cells during an infection with treatment at 54 hours after infection of 100 simulations with both techniques are shown. Dotted lines indicate the 1 standard deviation from the mean.

To illustrate the effect of different switching levels, 100 simulations are done with a switching level of only 10 cells and the same is done for a switching level of 10^4 cells. In the first case the hybrid simulation method is delayed with respect to the full Gillespie method. The reason is that the stochastic events in the slow part have less influence.

Setting the switching level to 10^4 overestimates the number of cells that get infected with resistant type, as it assumes that the amount of healthy cells is not influenced by the infections with resistant type until the switch to deterministic dynamics occurs. In the hybrid simulation method, the number of healthy cells is taken from the deterministic solution of the fast part and therefore does not include the dynamics of the slow part. For relatively low levels of resistance this is not a problem, but for higher levels the difference become large, as can be seen in Figure 4.13.

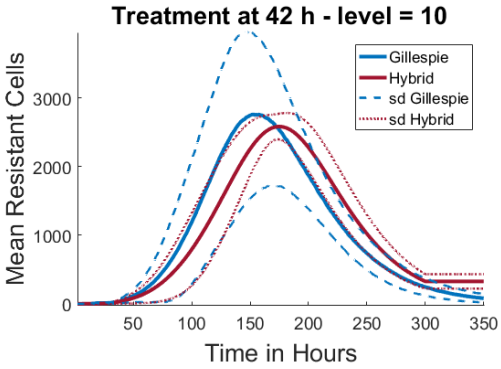

FIGURE 4.12: The means of the number of resistant cells during an infection with treatment at 42 hours after infection of 100 simulations with both techniques are shown for a switching level of 10.

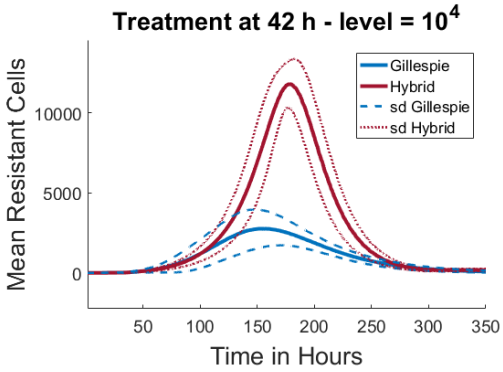

FIGURE 4.13: The means of the number of resistant cells during an infection with treatment at 54 hours after infection of 100 simulations with both techniques are shown for a switching level of 10^4.

The reaction rate of the empty reaction also influences the results of the comparison of both methods, as explained in the previous Section. To get insight in the different results for different reaction rates for treatment at 18 hours Figure 4.14 and 4.15 are shown. Figure 4.14 indicates that a reaction rate of zero accelerates the appearance of resistance, as the peak of resistance for the hybrid method finds itself before the peak of the full Gillespie algorithm. A very high reaction rate ($300 \quad h^{-1}$) increases the differences between both methods with respect to the results of a reaction rate of $90 \quad h^{-1}$, as can be seen in Figure 4.15.

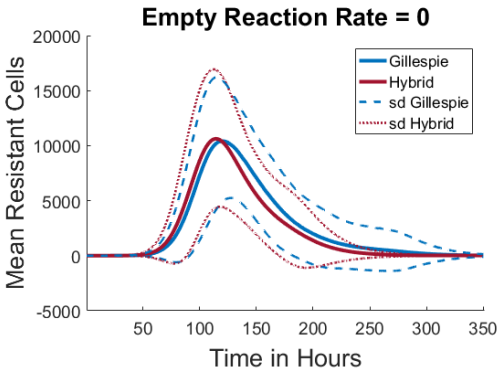

FIGURE 4.14: The means of the number of resistant cells during an infection with treatment at 18 hours after infection of 100 simulations with both techniques are shown for reaction rate for the empty reaction of 0.

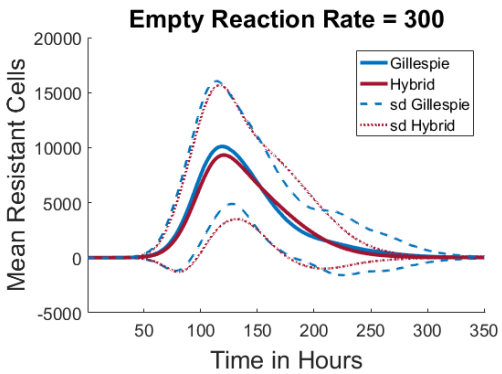

FIGURE 4.15: The means of the number of resistant cells during an infection with treatment at 18 hours after infection of 100 simulations with both techniques are shown for reaction rate for the empty reaction of 300.

Conclusion The results of the hybrid simulation method are extremely similar to the results of a full Gillespie version of the model. Hence, it can be concluded that the hybrid simulation method is a good technique to simulate the within-host model in a fast and efficient way. In order to obtain precise results, the choice of the switching level and (to a lesser extent) the reaction rate of the empty reaction are important.

Chapter 5

Linking the Within-host and Between-host Scales

The within-host model gives as output the dynamics of the infected cells of each type during the course of the infection. This information must now be incorporated into the between-host model. The duration of the infection for each patient can also be deduced from the results of the within-host model. Moreover, the total infectious load (the integral of the graph of the total number of infected cells over time) can be linked to the expected number of secondary infections caused by a primary infective. This number is called E_0. E_0 can be though of as the basic reproduction number of one patient, instead of the usual R_0 which indicates the basic reproduction number averaged over a whole group of patients.

However, how these two measures, the total infectious load and E_0, are related is not clear (Handel et al., 2013). Handel et al., 2013 present multiple options for the relationship: a linear relation, a Hill function or a logarithm of the total infectious load. They cannot confidently specify which of them would be the most appropriate to use. Nonetheless, they do argue that, based on biological arguments, a Hill function is most likely.

In the first instance, a linear link between the infectious load of a patient and E_0 is applied. The translation is made such that the E_0 of the healthy patients without treatment is equal to 1.5 as found in the literature (Fraser et al., 2009, Handel, Longini, and Antia, 2009). However, applying the same translation to the results of the resistant type strain leads to a E_0 value smaller than one. Although the reproduction number of the resistant type is expected to be smaller than the reproduction number of the sensitive type due to a cost in fitness for obtaining the resistance, it is still expected to be larger than one. The reason is that a value less than one would indicate that the resistant strain is not able to spread within a population, which is a contradiction to for instance the findings of Ferguson et al. (2003).

Furthermore, the linear translation results in a reproduction number higher than four for the elderly patients without treatment, which seems unreasonably high. Therefore, a linear relation between the total infectious load and the expected number of secondary infections is unlikely.

Biology suggests that a certain threshold value of infectiousness is necessary to be able to infect new patients. In addition, for very high values of infectious load fluctuations of E_0 are expected to be very small. A Hill function can capture this type of relation very well. Ferguson et al., 2003 estimated the constants for this equation for their model. Unfortunately, their infectious load is measured in a different way and

the model is different as well. Therefore, these constants cannot be used.

The constants that will be used in the model are chosen such that the E_0 of the healthy individuals is again equal to 1.5 on average, the E_0 of the healthy individuals infected with resistant type is slightly bigger than one and the E_0 of the elderly infected with sensitive type lies around 2. The E_0 values obtained from 1000 simulations of each type are shown in figure 5.1. The Hill function used to link the within and between-host model is;

$$y = \frac{(h_l x)^3}{5 + (h_l x)^3} + 1.1, \tag{5.1}$$

where $h_l = 5.5246 \times 10^{-10}$. The results of the Hill function are more realistic compared to the linear linking method and therefore this link is used for the model.

The probability that an individual infected with resistant type influenza infects a new person is smaller than the probability that an individual infected with sensitive type infects a new person. As can be seen in Figure 5.1, a smaller infectious load leads to a smaller E_0 value. This difference comes from the fact that the infectious period of cells infected with resistant type is smaller than for sensitive type. Therefore, the one cell infected with resistant type has a smaller contribution to the infectious load than a cell infected with the sensitive type.

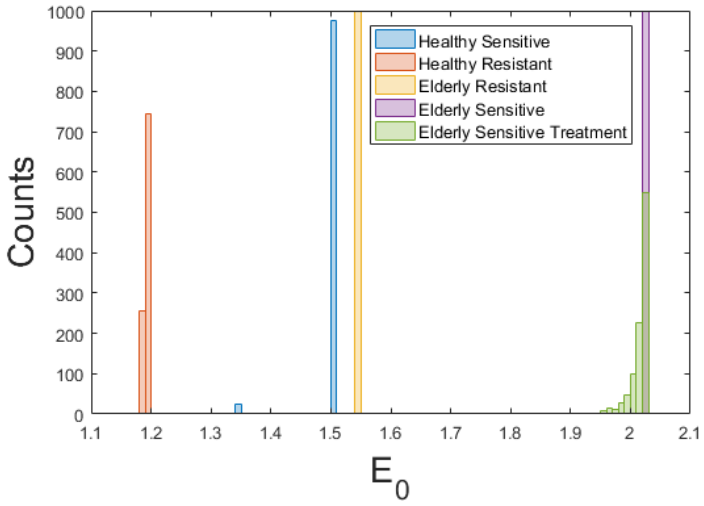

FIGURE 5.1: Histogram of E0 values for 1000 patients of each type.

In figure 5.1 the healthy individuals do not only have one big peak around 1.5, but also a smaller one around 1.35. The explanation for this is that in some cases (24 out of 1000) the resistant strain does come up, even though there is no treatment. The number of cells that get infected in these cases is very limited (as can be seen in Figure 5.3) but, the effect is large enough to result in a different E_0 value. The dynamics of the infection are shown in Figure 5.2 and 5.3 for examples where resistant does not come up and where it does.

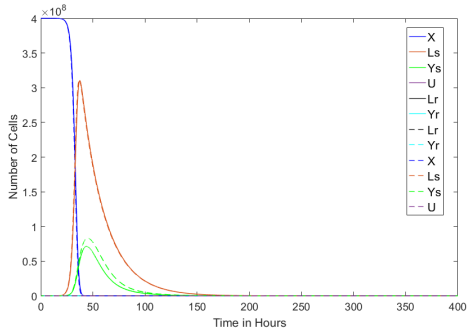

FIGURE 5.2: The dynamics of the within-host model without treatment. For the solid lines resistance did not come up, but for the dashed line it did.

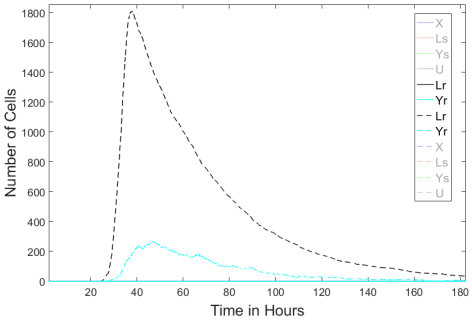

FIGURE 5.3: The dynamics of the slow part of the within-host model without treatment. For the solid lines resistance did not come up, but for the dashed line it did.

Chapter 6

Between-host Model

6.1 The Model

The previous chapter describes the link between the within-host scale model and the reproduction number in the between-host model. The ODE system in Equation 6.1 represents the between-host model. Notice that the basis for this model is a standard SIR model. There are five different categories in the model: susceptibles (S), patients infected with the sensitive strain (I_s), patients infected with the sensitive strain undergoing treatment (I_s^t), patients infected with the resistant strain (I_r) and individuals that have recovered (R). N is the total number of people in the population. A graphical version of the model is shown in Figure 6.1.

Each category is divided in two types; elderly and health care workers (HCWs). The linkage between these two groups is given by a contact matrix, which indicate the contact rate between the groups and within the groups. The treatment rate (σ) is different for the elderly than for the HCWs. How this is incorporated in the model is explained in the next section.

The parameters that define the behaviour of the between-host model are: infection rate of the sensitive type (α_s), infection rate of the sensitive type under treatment (α_r), infection rate of the resistant type (α_r), probability that a new infection caused by a patient under treatment is with resistant strain (p), treatment rate (σ), rate of recovery for sensitive strain (η_s), rate of recovery for resistant strain (η_r) and rate of recovery under treatment for sensitive strain (η_t).

$$\dot{S} = -\frac{\alpha_s}{N} S I_s - \frac{\alpha_r}{N} S I_r - \frac{\alpha_t}{N} S I_s^t \tag{6.1a}$$

$$\dot{I}_s = \frac{\alpha_s}{N} S I_s + (1-p)\frac{\alpha_t}{N} S I_s^t - \sigma I_s - \eta_s I_s \tag{6.1b}$$

$$\dot{I}_s^t = \sigma I_s - \eta_t I_s^t \tag{6.1c}$$

$$\dot{I}_r = \frac{\alpha_r}{N} S I_r + p\frac{\alpha_t}{N} S I_s^t - \eta_r I_r \tag{6.1d}$$

$$\dot{R} = \eta_s I_s + \eta_t I_s^t + \eta_r I_r \tag{6.1e}$$

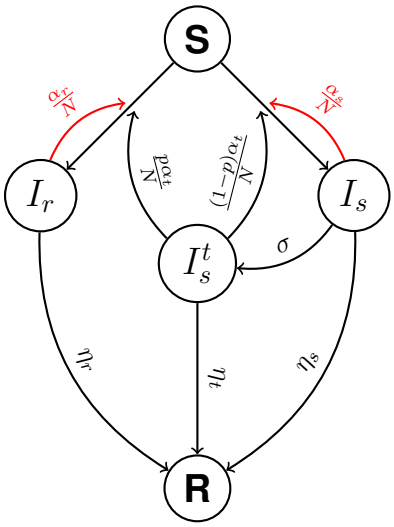

FIGURE 6.1: Overview of the between-host model. The red arrows indicate that the groups at the origin influence the rate of the arrow it points towards.

The E_0 value obtained from the within-host model can be included in this model as $E_0 = \frac{\alpha}{\eta}$ for each type. η_r, η_t, η_s and p are given by the output of the within-host model and therefore vary for each patient. Thus, α can be found by using the result of the within-host model for η and E_0. σ and N can be chosen as required for each simulation. The next section explains how the output from the within-host model is used to find these parameters in the between-host model.

6.2 Simulation of the full Model

Simulating a complete within-host model each time a new person gets infected in the between-host model takes much computation time. Therefore, a database of patients is made for each type. During the simulation of between-host model a random sample from the database is chosen with replacement for every new infection.

At time $t = 0$ one person is infected. The E_0 of this person is calculated by applying the Hill function to the infectious load of the within-host model for the patient. From a geometric distribution with mean E_0 (the number of new infections by this first infective) is calculated. The timing of these new infections is chosen according to the distribution of the Hill function over the infectious load in time.

For each new infective the type of person (elderly or HCW) is chosen based on the contact matrix and the number of susceptibles that is left in each group. The newly infected person can get infected with either type of virus strain. The probability to get infected with resistant type (p) is given by the number of resistantly infected cells divided by the sum of the number of sensitively infected cells and the number of resistantly infected cells in the output of the within-host model at the time when the initially infective infects the new person.

Note that, although this possibility is not included in the model, someone from group I_s can also infect a susceptible with resistant type. However, this probability is

negligible small, as the only cells that are infected with resistant type for the within-host model of a patient without treatment come directly from mutation events, and there are thus only a limited amount of them.

An infective is considered to be recovered if the total number of infected cells in the within-host model is smaller than 1.88×10^6. Recovered individuals are assumed to be immune for the infection and therefore do not return to the susceptible state.

In the case where vaccination is applied to (part of) the population an extra step is taken after the new infections took place. The probability that the new infective is vaccinated is multiplied with the probability that the vaccine is effective. With this probability the infection does not take place and is removed from the simulation.

6.3 Comparing the model with Gillespie version of the model

In order to validate the method of modeling, a simplified version of the model is compared with a full Gillespie version of itself. In this simplified model all patients are the same. They all have the same basic reproduction number (R_0^s): 1.5 when they are infected with sensitive type and 1.1 when they are infected with resistant type (R_0^r). The time of the infection (γ) is set to 120 hours for both types.

The treatment rate is set to 0.6 and the probability that a person under treatment infects a new person with resistant type (p) is set to 0.1.

This is equivalent to a Gillespie algorithm with the following reactions:

$$S + I_s \rightarrow I_s, \tag{6.2}$$
$$S + I_s \rightarrow I_r, \tag{6.3}$$
$$S + I_r \rightarrow I_r, \tag{6.4}$$

and ignoring the reactions of recovery, as they do not influence the results. The rates for these reactions are respectively; $(1-p)\frac{R_0^s}{\gamma} = \frac{0.9 \times 1.5}{120}$, $p\frac{R_0^s}{\gamma} = \frac{0.1 \times 1.5}{120}$ and $\frac{R_0^r}{\gamma} = \frac{1.1}{120}$.

With the use of the simplified version of the simulation method described above, in 59.9 % of the cases no resistance appears, while in the Gillespie version this is 59.5 % of the cases. Testing the difference between those two numbers with a binomial test results in a p-value of 0.5448, thus it can be assumed that they are equal. The distributions of the number of people that got infected with resistant type during an epidemic in which resistance does appear are shown in Figure 6.2. The p-value for a Mann-Whitney U test to check if both histograms originate from the same distribution is 0.3097. Therefore, it can be concluded that the distributions are practically the same.

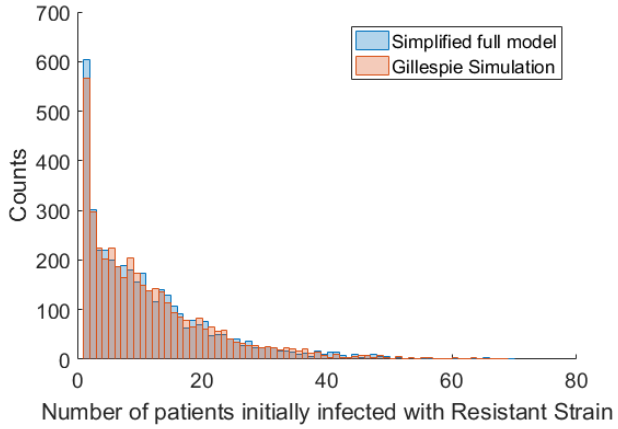

FIGURE 6.2: Histogram of number of resistant infections for 1000 simulations of the simplified version of the full between model and the Gillespie version of the model.

Besides comparing the number of people that get infected with resistant type, also the distributions of the total final sizes are compared. These distributions are shown in Figure 6.3. The p-value for a Mann-Whitney U test is 0.4526, therefore it can be assumed that the distributions are similar. In conclusion, the simulation method described in this chapter works as desired, because the results are similar to a full Gillespie Algorithm. On average, one simulation of the simplified full model takes 3.269×10^{-3} s and the Gillespie Algorithm takes 1.360×10^{-3} s.

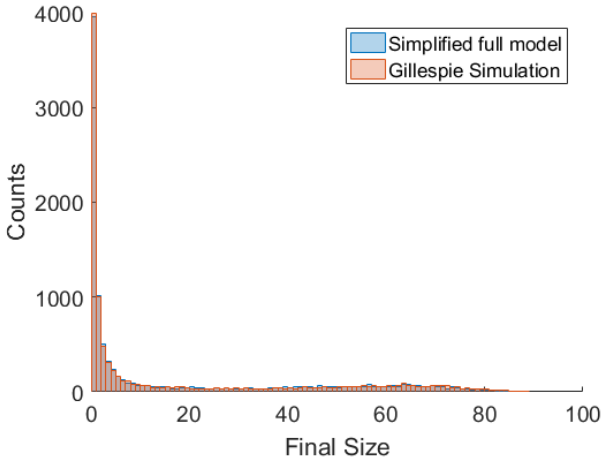

FIGURE 6.3: Histogram of final size for 1000 simulations of the simplified version of the full between model and the Gillespie version of the model.

Chapter 7

Results

The five research objectives described in the introduction have been researched with the model that is described in the previous chapters. The results are summarized in this chapter. First the results of the within-host model and then observations from the full model.

7.1 Within-host Model

7.1.1 Effect of Treatment Timing

The outputs of the within-host model for different treatment times are shown in Figures 7.1 to 7.7. Below, they will be used to explain the the probability that drug-resistant viruses appears during treatment at different times. These probabilities are shown in Figure 7.9. Note that the output figures are the outputs of just one simulation for each treatment time and as the model is stochastic, all simulations will look different. In Figures 7.1 to 7.7 resistance does not occur. A simulation in which resistance did occur is shown in Figure 7.8.

Figure 7.1 and 7.2 make clear that treatment at 15 or 20 hours can prevent an infection from taking place. Only very few healthy cells get infected with the virus in this case. As a result, the probability that resistance appears for very early treatment is relatively low, as can be seen in Figure 7.9. The reason is that if only few reactions of infection took place before treatment, the probability that a resistant type virus has appeared before the start of treatment is small. If there are no resistant cells at the start of treatment, they can not appear at all, as in the simulation the probability of

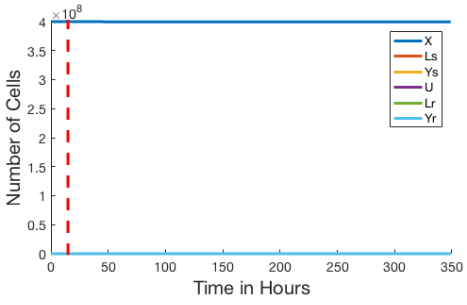

FIGURE 7.1: Evaluation of within-host model for treatment in a healthy person infected with sensitive strain influenza at 15 hours after infection.

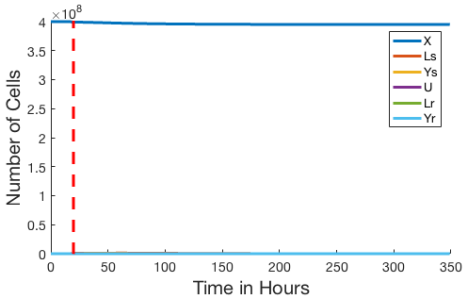

FIGURE 7.2: Evaluation of within-host model for treatment in a healthy person infected with sensitive strain influenza at 20 hours after infection.

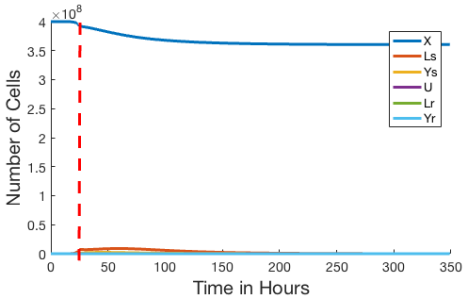

FIGURE 7.3: Evaluation of within-host model for treatment in a healthy person infected with sensitive strain influenza at 25 hours after infection.

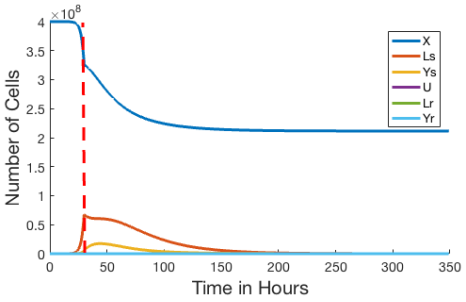

FIGURE 7.4: Evaluation of within-host model for treatment in a healthy person infected with sensitive strain influenza at 30 hours after infection.

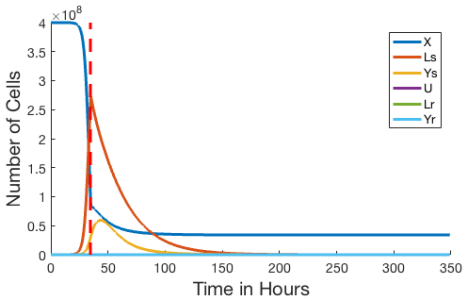

FIGURE 7.5: Evaluation of within-host model for treatment in a healthy person infected with sensitive strain influenza at 35 hours after infection.

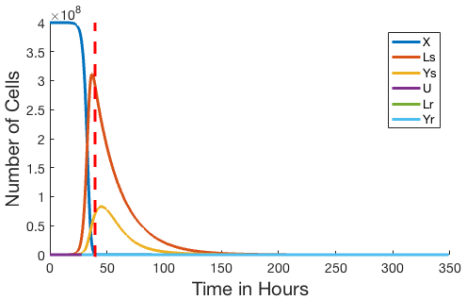

FIGURE 7.6: Evaluation of within-host model for treatment in a healthy person infected with sensitive strain influenza at 40 hours after infection.

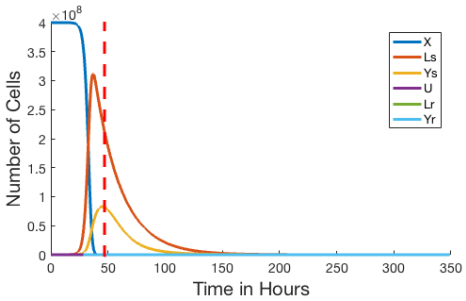

FIGURE 7.7: Evaluation of within-host model for treatment in a healthy person infected with sensitive strain influenza at 45 hours after infection.

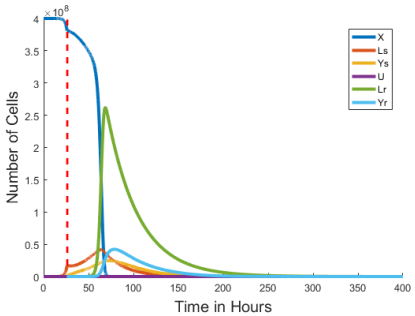

FIGURE 7.8: Evaluation of within-host model in an elderly person that is under treatment starting at 25 hours after infection (indicated by the red line).

appearance is set to zero after treatment.

On the other hand, if a resistant cell has appeared before treatment, it has a lot of opportunities to spread, as many healthy cells are available to infect. This is supported by Figure 7.10, which shows that the probability of not finding any resistance is almost one for early treatment. This implies that almost every time that a resistance cell appears more than 50 % of the cells get infected with resistant type. To be precise, for treatment at 15 hours: of the 1000 simulations 999 did not show any resistant cells. In the only case that resistance occurred, 99.5 % of the cells became infected with resistant type virus. For treatment at 20 hours, 988 cases did not show any resistance, but in 10 cases more than 50 % of the cells were infected with resistant type virus.

Figure 7.9 shows that the highest probability for the appearance of resistant strain influenza is found for treatment at 25 hours. In this situation more cells are infected with sensitive type before the start of treatment than for earlier treatment. Therefore, the probability that there is at least one cell infected with the resistant type strain at the start of the treatment is higher. Additionally, there are still a lot of healthy cells alive at the start of treatment. Thus, the resistant infected cell has a lot of opportunities to infect others and spread within the host.

The probability of resistance for treatment at 30 hours is seen to be zero in Figure 7.9. None of the simulations showed that more than 50 % of the cells were infected with resistant type. However, of the 1000 simulations for treatment at 30 hours only in 327 cases was the fraction of cells infected with resistant type zero. In other words, the probability that none of the infections develops with resistant type is 67.3 %, as shown in figure 7.10. Thus, resistance does appear relatively often, but not for more than half of the eventually infected cells.

It is important to note that even though the probability that at least 50 % of the cells is infected with resistant type is zero, an individual treated at 30 hours can infect others with resistant type. This originates from the fact that the probability that a new onward infection is of the resistant type is the ratio of cells infected with resistant type to the total number of infected cells from the within-host model at the time of the infection. The mean fraction of cells infected with resistant type for treatment at 30 hours is 0.0249. This results in an average probability of 0.0249 that a new infection is with resistant type for individuals treated at 30 hours. Therefore, drug-resistance can still spread in an epidemic with consistent treatment at 30 hours.

For treatment at 35 hours and later, the opportunities for spread of the resistant strain after treatment have decreased even further, as almost all healthy cells are already infected or dead. Furthermore, it can be seen in Figure 7.10 that the probability that no cell gets infected with resistance is almost zero. This is a result of the fact that a lot of cells get infected with sensitive strain and for each of these reactions the probability that resistance occurs is μ. So if the number of reactions increases, this probability converges to one. So, the probability to find some cells infected with resistant type is almost one, however, the probability that a patient treated at 35 hours or later infects a susceptible with resistant type is very close to zero.

Conclusion It can be concluded that the probability that at least one cell gets infected with resistant type influenza increases with a later treatment time. However, the probability that a resistant cell gets the opportunity to spread such that at least 50 % of the cells get infected with resistant strain decreases with later treatment times. Therefore, there exist an optimal treatment time for the appearance of resistant type influenza, which lies around 30 hours after infection.

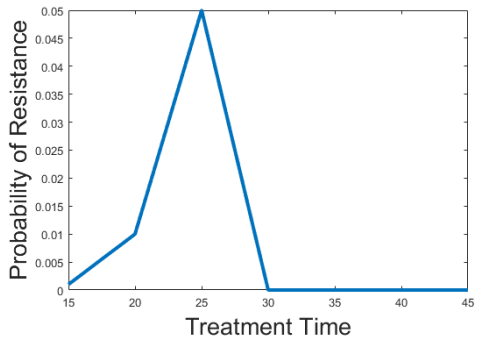

FIGURE 7.9: Probability that more than 50 % of the infected cells are infected by resistant strain influenza as a function of treatment time.

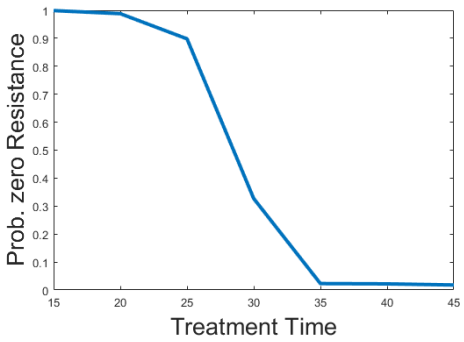

FIGURE 7.10: Probability that 0 cells are infected with resistant type cells during the infection.

7.2 Between-host Model

Each simulation starts with 250 elderly individuals and 50 HCWs. Together they represent an old people's home. The contact rate between the elderly persons is fixed at 25 day^{-1}. Also, the contact rate between the health care workers is set to 25 day^{-1}, since we can assume that both the elderly and health care workers have much contact between themselves. The contact rate between HCWs and elderly persons is assumed to be smaller and therefore set to 10 day^{-1}. Moreover, the contacts are assumed to be symmetric, hence the contact matrix is symmetric. Unless otherwise indicated, the initial infective is an elderly person and the treatment time is log-normal distributed around 32 hours with a standard deviation of 6 hours. In addition, the treatment rate is fixed at 0.6 per case for all elderly persons except when the effect of the treatment rate is tested.

An epidemic is classified as minor when less than 50 individuals get infected. All other sizes of epidemics are considered to be a major outbreak. To compare the effects of different initial conditions and treatment/vaccination strategies five different measures are compared. These measures and the way in which they are compared are summarized in Figure 7.11.

The effects of the different strategies on the number of infections in the elderly and/or resistant groups are measured by comparing fractions. This is chosen to eliminate the influence of differences in final size, as they are already evaluated. To give a complete picture of the obtained data, box-plots of the distributions of the absolute number of infections in each group within a major outbreak are shown in Appendix A. Moreover, as our main interest is in protecting the elderly people from

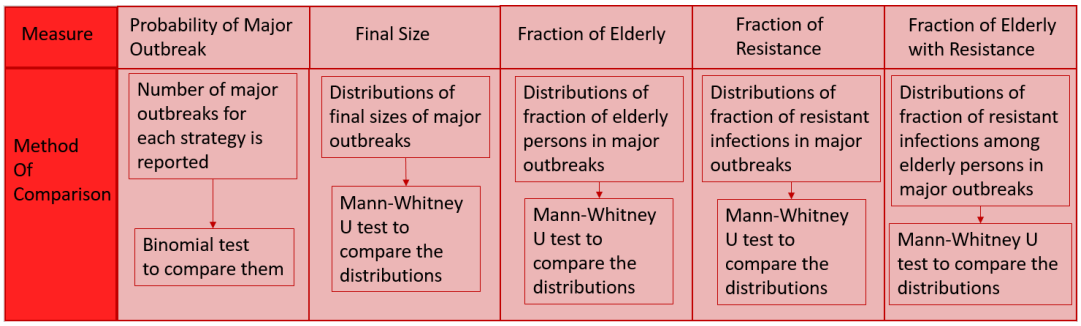

FIGURE 7.11: Overview of the evaluated measures and techniques for comparison of different strategies.

an infection with resistant type, a box-plot for the number of elderly infected with resistant type is reported for all cases.

7.2.1 Effect of initial condition

In this section, simulations starting with an infected elderly person are compared with simulations starting with an infected HCW. Out of 1000 simulations, 496 resulted in a major outbreak when the first infective was an elderly person and 387 major outbreaks occurred when the first infective was a HCW. The difference is significant with a p-value of 9.1851×10^{-7}.

This observation can be easily explained. As the E_0 value is higher for the elderly than for the HCWs, the probability that the first infective infects at least one person is thus higher when it is an elderly person. Moreover, due to the contact matrix the probability that the next infective is again an elderly person is higher if the first one was an elderly person, therefore, the probability that this infective infects at least one new person is higher again. This reasoning repeats itself when the second infective is an elderly person as well. Hence, especially at the start of an epidemic, the number of infections is higher when the initial infective is an elderly person.

A Mann-Whitney U test to compare the distributions of the final size of the major outbreaks leads to a p-value of 0.1974, indicating that it can be assumed the distributions are equal. A histogram of both distributions is shown in Figure 7.12.

In Figure 7.13 a histogram of the fraction of elderly people infected during a major outbreak is shown for both cases. The p-value for a Mann-Whitney U test comparing these distributions is 1.03×10^{-9}. Therefore, it can be said that there is a significant difference in the fraction of infections that are among elderly people. Of course, this is as expected, because the probability that an elderly person infects an other elderly person is higher than the corresponding probability for a HCW. Hence, the distribution of the fraction of a major outbreak that is elderly is more shifted to the right.

The fraction of people infected with resistant type influenza in the major outbreaks is not significantly different between both situations; the p-value thereof is 0.1439. The histogram of these distributions is shown in Figure 7.14.

The distribution of the fraction of resistant infections among elderly people is also not significantly different for both situations. The p-value is equal to 0.1919 in

this case. Figure 7.15 represents the distributions. Figure 7.18 represents the distributions of the absolute number of elderly persons infected with resistant type influenza for both initial conditions. These distributions are significantly different from each other, due to the influence of the number of major outbreaks and the fraction of total infections that is among elderly people, both mentioned before (p-value = 4.7156×10^{-8}). The mean for the case in which an elderly person is the initial infective is 10.85 and for the situation of an initial infective of a HCW is 7.4360.

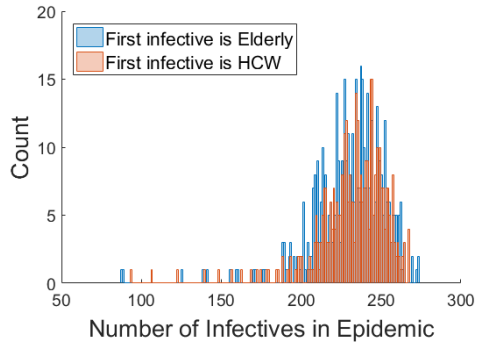

FIGURE 7.12: Histogram of the number of infectives in major outbreaks when the first infective is either an elderly or a HCW.

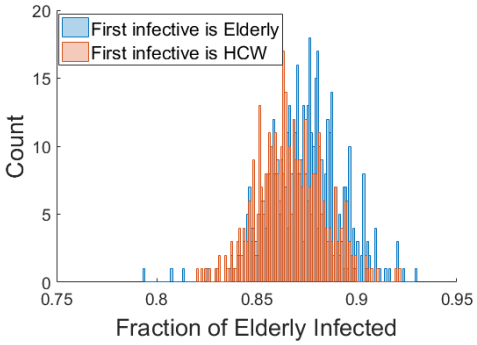

FIGURE 7.13: Histogram of the fraction of infectives in major outbreaks that is elderly when the first infective is either an elderly or a HCW.

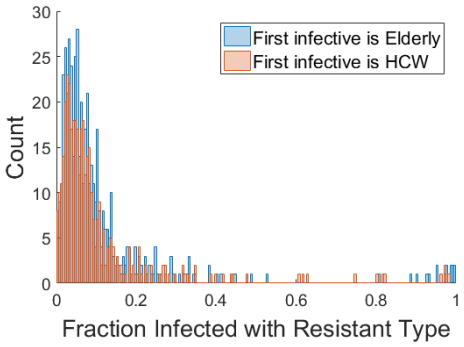

FIGURE 7.14: Histogram of the fraction of infectives in major outbreaks that is infected with resistant strain when the first infective is either an elderly or a HCW.

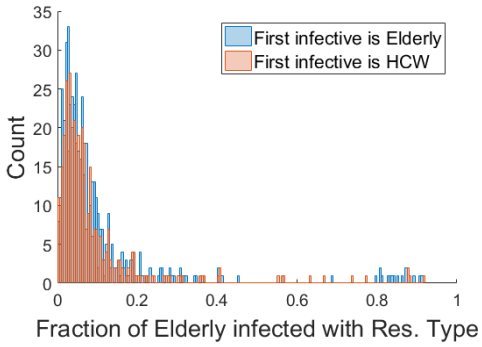

FIGURE 7.15: Histogram of the fraction of infectives in major outbreaks that is elderly and infected with resistant strain when the first infective is either an elderly or a HCW.

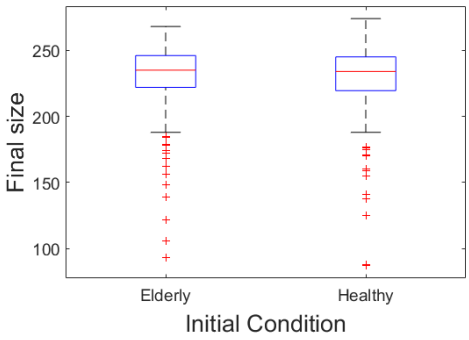

FIGURE 7.16: Box-plot of size of final outbreaks of major outbreaks of 1000 simulations. The means for respectively an elderly as initial infective and an HCW as initial infective are 230.42 and 231.67. The medians are 234 and 235 respectively.

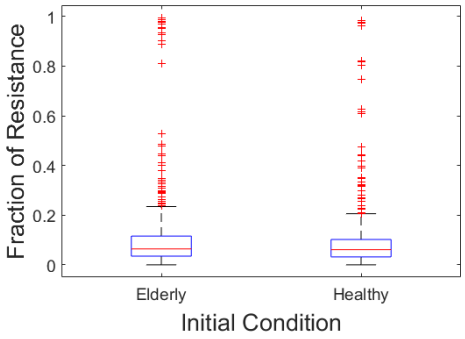

FIGURE 7.17: Box-plot of fraction of resistant infections of final outbreaks of major outbreaks of 1000 simulations. The means for respectively an elderly as initial infective and an HCW as initial infective are 0.1154 and 0.1010. The medians are 0.0640 and 0.0621 respectively

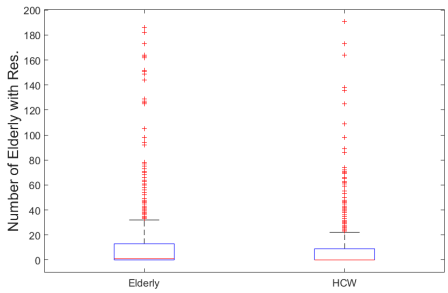

FIGURE 7.18: Box-plot of number of elderly infected with resistant type during an epidemic for both initial conditions.

Conclusion The probability of a major outbreak is larger when the initial infective is an elderly person. The distribution of the final size of major outbreaks does not differ between the different initial conditions. Moreover, the fraction of infections that suffer from an infection of resistant type does not differ. On average, more elderly persons get infected with resistant type influenza when the first infective is an elderly person.

7.2.2 Effect of vaccination

Two different vaccination strategies are compared. In the first case 80 % of the elderly people are vaccinated. The efficacy of the vaccine in an elderly person is set to 20 %. In the second situation 80 % of the health care workers are vaccinated with an efficacy of 80 %. Vaccinating the elderly people leads to 398 major outbreaks in 1000 simulations and vaccinating the HCWs leads to 429 major outbreaks. This difference is not significant: the p-value is equal to 0.1593.

The distribution of the final size of the major outbreaks of both vaccinating strategies are shown in Figure 7.19 and 7.20. A box-plot of both distributions can be found in Figure 7.25. The distributions are significantly different, which follows from a Mann-Whitney U test with a p-value of 1.35×10^{-4}. Obviously, the distributions for the fraction of infections in major outbreaks among elderly people is different as well, the p-value thereof is 4.01×10^{-133}. These distributions are shown in Figure 7.21.

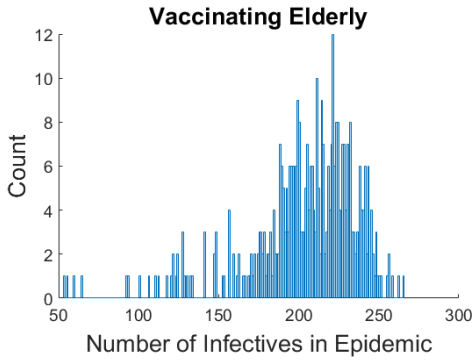

FIGURE 7.19: Histogram of the final size of major outbreaks where the elderly are vaccinated.

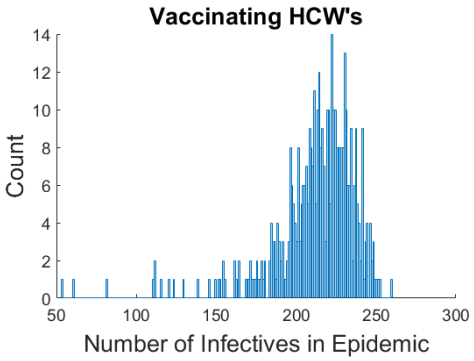

FIGURE 7.20: Histogram of the final size of major outbreaks where the HCWs are vaccinated.

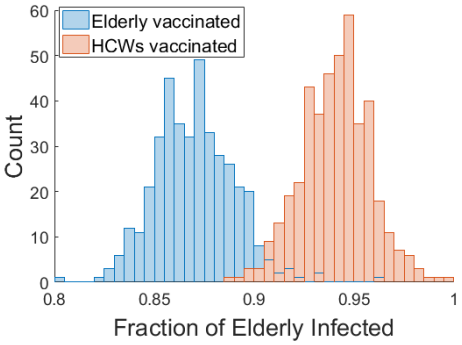

FIGURE 7.21: Histogram of the fraction of infections in major outbreaks that is elderly when either the elderly or the HCWs are vaccinated.

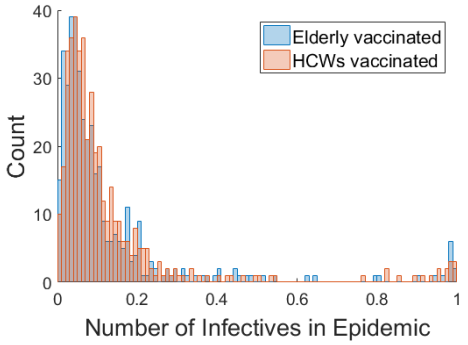

FIGURE 7.22: Histogram of the fraction of infectives in major outbreaks that is infected with resistant strain when either the elderly or the HCWs are vaccinated.

The p-value for testing the difference between the distributions of the fraction of people infected with resistant type in major outbreaks is 0.0342. As can be seen in Figure 7.22 the strategy to vaccinate the HCWs results in a slightly higher fraction of resistant cases. This can be explained by the fact that more elderly people get infected with this strategy, and therefore more treatment is applied and the probability that resistant type occurs is higher. The differences in mean can be found in Figure 7.26.

Similar reasoning as above can be used to explain the difference in distribution of the fraction of the resistant infections among elderly people. These distributions are shown in Figure 7.23 and the p-value for the difference is 0.0024. The distributions of the absolute number of elderly persons that got infected with resistant type are

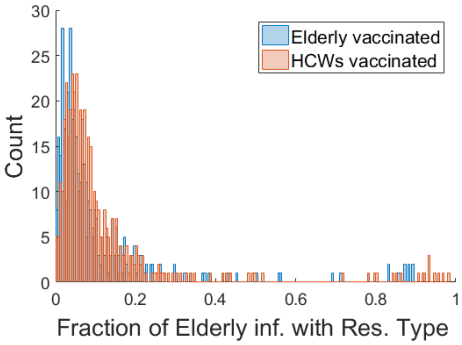

FIGURE 7.23: Histogram of the fraction of infectives in major outbreaks that is infected with resistant strain when either the elderly or the HCWs are vaccinated.

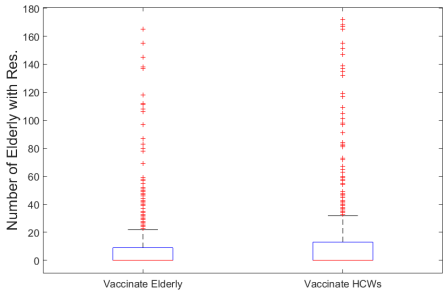

FIGURE 7.24: Box-plot of number of elderly infected with resistant type during an epidemic for both initial conditions.

shown in Figure 7.24. The mean for vaccinating the elderly people is 7.77, where vaccinating the HCWs results in 10.32 elderly people infected with the resistant type on average. The distributions are found to be different with a p-value of 0.0070.

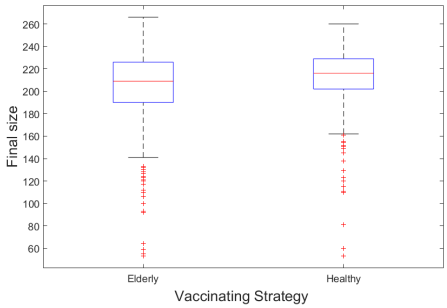

FIGURE 7.25: Box-plot of size of final outbreaks of major outbreaks of 1000 simulations. The means for respectively vaccinating elderly and HCWs are 203.28 and 211.75. The medians are 209 and 216 respectively.

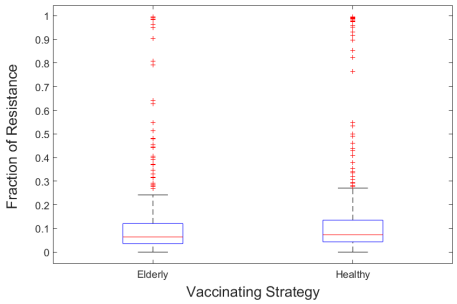

FIGURE 7.26: Box-plot of fraction of resistant infections of final outbreaks of major outbreaks of 1000 simulations. The means for respectively vaccinating elderly and HCWs are 0.1218 and 0.1301. The medians are 0.0642 and 0.0735 respectively.

Conclusion Vaccinating the elderly leads on average to smaller number of major outbreaks and to less resistant infections than vaccinating the HCWs. Therefore, vaccinating the elderly is the better strategy. However, this conclusion is also influenced by the fact that the total vaccinating coverage is higher when vaccinating the elderly, as they comprise a larger part of the population. On average, 40 people are protected from getting infected for the first vaccinating strategy ($0.8 \times 0.2 \times 250$) and 32 people when the HCWs are vaccinated ($0.8 \times 0.8 \times 50$).

7.2.3 Effect of treatment timing

The effects of treatment timing at the within-host level (Section 7.1.1) affect the results of the full model as well. The different treatment times that are compared are; 15, 20, 25, 30, 35, 40 and 45 hours after the start of the infection. In this situation treatment is applied exactly at the treatment time and not distributed around this time. Table 7.2 reports the number of major outbreaks for each treatment time.

To judge the difference in the probability of a major outbreak, the p-values of all combinations of treatment times are shown in Table A.1. From these p-values it can be concluded that the number of major outbreaks is significantly smaller for treatment at 15 hours compared to any other treatment time. The same is true for treatment at 20 hours. All other number of major outbreaks are not significantly different from each other. These observations can be explained with the results of the within-host analysis of Section 7.1.1. Figure 7.1 and 7.2 show that treatment at 15 and 20 hours basically prevent the infection to take place, therefore, the probability to infect others is very small when treatment is applied this early, resulting in a lower probability of a major outbreak. Treatment at later times (from 25 hours up to 35 hours), reduces the infectious load, but does not prevent an infection.

TABLE 7.1: Number of major outbreaks for different treatment times.

Treatment time (hours)	15	20	25	30	35	40	45
Number of major outbreaks	304	417	478	462	501	489	503

A box-plot of the distributions of the final sizes of the major outbreaks of 1000 simulations is shown in Figure 7.27. This figure makes clear that the final size increases with the treatment time. However, after 35 hours, treatment no longer influences the final size. Table A.2 shows the mean and median values for each distribution of the final size of major outbreaks as well as the mean and median of the fraction of infections of the major outbreak that is with resistant type.

A Mann-Whitney U test is performed for each combination of treatment times to check that the distributions are indeed different. The p-values for these tests can be found in Table A.3. These p-values indicate that the distributions of all treatment sizes are different, except for treatment at 35, 40 and 45 hours. Moreover, the distributions for 25 and 30 hours are equal. A selection of the distributions is shown in Figure 7.29.

For the distribution of the fraction of infections that are of resistant type, the only distributions that correspond to each other are at 15 and 35 hours and between treatment at 40 and 45 hours. All p-values are summarized in Table A.4.

Using Figure 7.27, Figure 7.28 and the observations described above, it can be concluded that the final size of a major outbreak increases with the treatment time. However, the fraction of the people that is infected with resistant type increases for the first 4 treatment times and is almost zero afterwards. This observation is a direct result of the probabilities of appearance of resistant virus during the within-host model. A higher probability of appearance (more than 50 % of the cells are infected with resistant type) results in a higher fraction of resistant infections.

However, note that the highest fraction of resistance does not correspond to the highest probability of appearance. The explanation can be found in Subsection 7.1.1. In a lot of cases where treatment is applied at 30 hours the resistance appears, but is responsible for only a limited fraction of the infected cells. Therefore, they are not counted in Figure 7.9, but the probability that they spread resistant type virus is significantly larger than zero.

The differences between the distributions of the fraction of the major outbreak that is among elderly people are smaller. The p-values for this are shown in Table A.6. Moreover, the differences in distributions of the fraction of the resistant infections that is an elderly person are tested and the results are shown in Table A.7. Box-plots of these distributions for both measures are shown in Figure 7.31 and 7.32. Moreover, the mean and median values of the distributions for both measures are given in Table A.5.

A selection of the distributions of the fraction of elderly that gets infected during a major outbreak are significantly different, however, the differences in mean and median are very minimal. This is illustrated in Figure 7.30.

Figure 7.32 has to be treated with some care, as it does not show the cases in which no observations of elderly persons infected with resistant type were made. This results in $\frac{0}{0}$ for the fraction of resistant cases that is among elderly people. Table A.5 makes clear that in a lot of cases the median value is to not observe an elderly infected with resistance. Calculating the mean is not possible if in at least one case no observations were made. The only situation in which every simulation has at least one elderly infected with resistant type is for treatment at 30 hours. This is in agreement with the observation that for treatment at 30 hours results in the highest fraction of resistance. Figure 7.33 gives a better overview of the number of elderly persons infected with resistant type influenza. It is very similar to Figure 7.28.

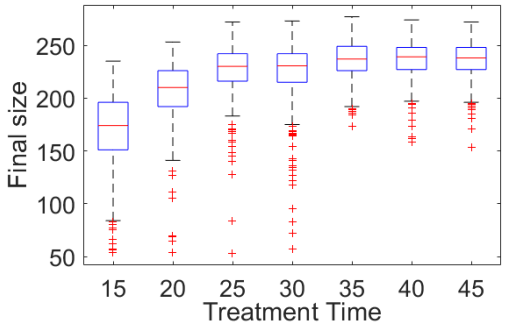

FIGURE 7.27: Box-plot of the final size major outbreaks of 1000 simulations for different treatment times.

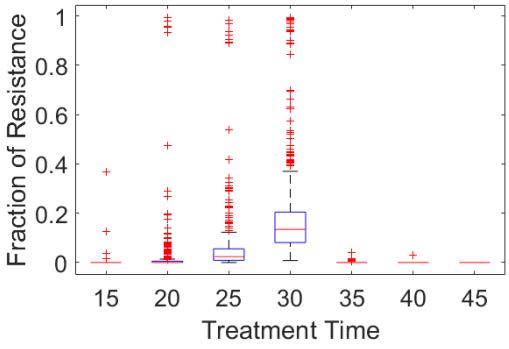

FIGURE 7.28: Box-plot of the fraction of resistant infections in major outbreaks of 1000 simulations for different treatment times.

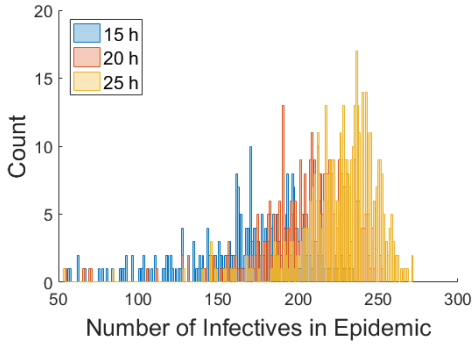

FIGURE 7.29: Histogram of the final size of major outbreaks of 1000 simulations of the between-host model for different treatment times.

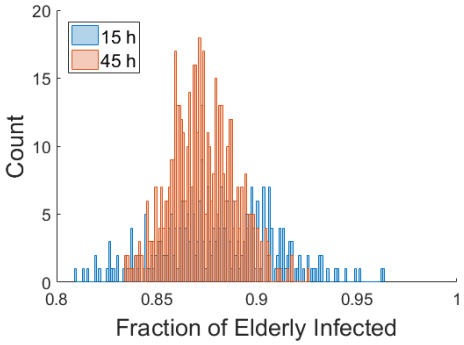

FIGURE 7.30: Histogram of the fraction of elderly infected in major outbreaks of 1000 simulations for different treatment times.

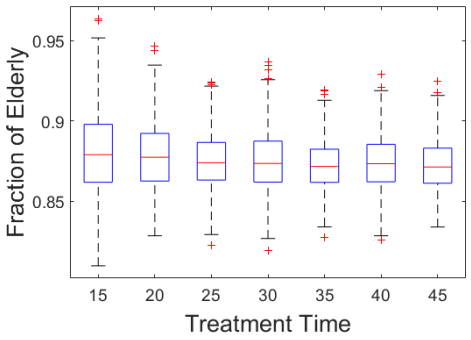

FIGURE 7.31: Box-plot of the fraction of infections in major outbreaks that is elderly of 1000 simulations for different treatment times.

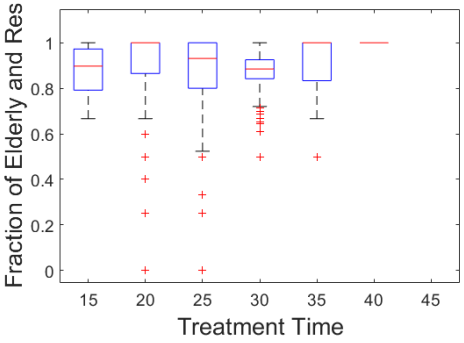

FIGURE 7.32: Box-plot of the fraction of infections in major outbreaks that is elderly and with resistant type in major outbreaks of 1000 simulations for different treatment times.

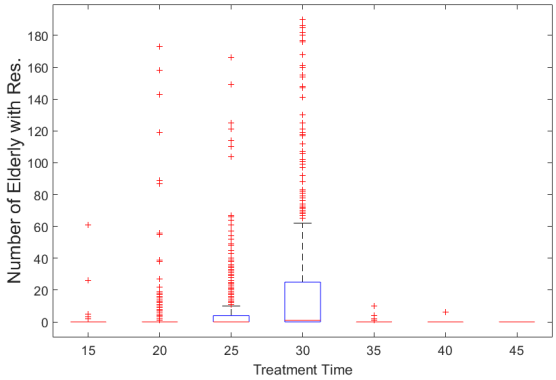

FIGURE 7.33: Box-plot of number of elderly infected with resistant type during an epidemic for all treatment times.

Conclusion Early treatment (15 hours after infection) is ideal, as it will decrease the probability of a major outbreak as well as the final size of the outbreak. Moreover, it does not yield a high fraction of resistant infections. However, treatment at 20, 25 and 30 hours after infection results in a decrease in final size, but an increase in the fraction of resistant infections. Especially treatment at 30 hours is highly inadvisable, as it leads to the highest fraction of resistant infections compared to all other treatment times.

7.2.4 Effect of Treatment Rate

Here, the effect of different treatment times is evaluated. The treatment times that are compared are: 0, 0.1, 0.2, 0.3, 0.4, 0.5, 0.6, 0.7, 0.8, 0.9 and 1. The number of major outbreaks for all treatment rates are given in Table 7.2. The p-values for testing the differences between these observations are shown in Table A.8. Only five of these p-values are significant; the comparison of a rate of 0.1 with a rate of 0.9 and the combination of a rate of 1 with 0.1, 0.4, 0.6 and 0.8. It can therefore be concluded that the probability of a major outbreak is slightly smaller for a treatment rate of 1. This is not surprising, as a higher treatment rate reduces the average E_0 and thus the spread within the population. However, the difference is small.

The p-values of the results of Mann-Whitney U tests for all different combinations of treatment rates (Table A.10) show that the distributions of most final sizes of major outbreaks are different. Figure 7.34 and Table A.9 show that the differences in the mean and distribution. This is illustrated by Figure 7.36 and 7.37 as well. The variance in the distributions is higher for higher treatment rates.

The differences among the distributions of the fractions of major outbreaks of resistant type is more obvious. Almost all p-values for differences between these distributions are significant, see Table A.11. Figure 7.35 and Table A.9 make clear that there is also a difference in the mean of these distributions. The fraction of resistance in major outbreaks increases for higher treatment rates. The reason is that resistance is far more likely to appear under treatment, more treatment gives thus more possibilities for appearance of resistance. If there is no treatment, resistance does not appear.

TABLE 7.2: Number of major outbreaks of 1000 simulations for different treatment rates.

Treatment Rate	0	0.1	0.2	0.3	0.4	0.5	0.6	0.7	0.8	0.9	1
Number of major Outbreaks	500	521	503	487	508	501	510	480	518	477	464

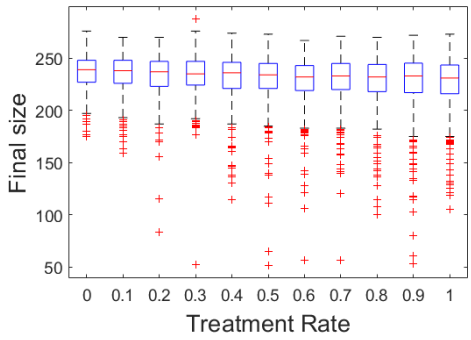

FIGURE 7.34: Box-plot of the final size of major outbreaks of 1000 simulations of between-host model for different treatment rates.

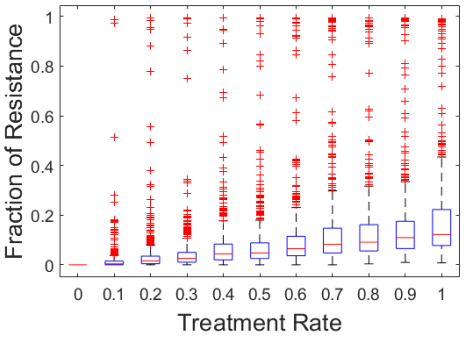

FIGURE 7.35: Box-plot of the fraction of resistant infections in major outbreaks of 1000 simulations of between-host model for different treatment rates.

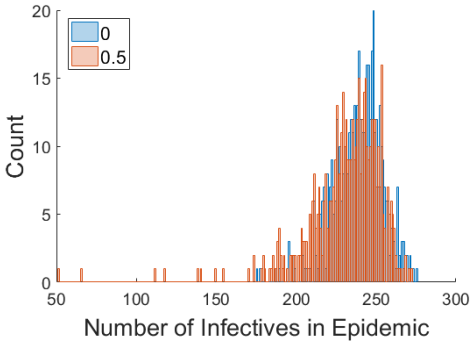

FIGURE 7.36: Histogram of number of infections in major outbreaks of 1000 simulations for treatment with rate 0 and 0.5.

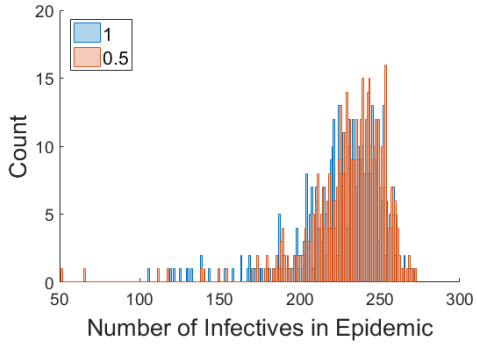

FIGURE 7.37: Histogram of number of infections in major outbreaks of 1000 simulations for treatment with rate 0.5 and 1.

Figure 7.38 shows a box-plot of the distributions of the fraction of elderly in major outbreaks for different treatment rates. The means and medians of these distributions are summarized in Table A.12 and the p-values for differences in the distributions can be found in Table A.13. Most significant values appear in the last column and indicate that treatment with rate 1 is different from all other treatment rates. The difference between the mean of the distributions for all treatment rates are small.

The distributions of the fraction of resistant infections in a major outbreaks that is elderly are shown in Figure 7.39. These distribution have to be treated with care again, as cases without observations of elderly infected with resistant type are not shown. In a major part of the cases no observations of this kind were made. This is due to the fact that for low treatment rates the fraction of resistance is low as well, the probability to find resistant cases in elderly is thus small. The means and medians of these distributions are summarized in Table A.12. However, too many data-points are missing to draw any definite conclusions from these observations. Therefore, Figure 7.40 contains box-plots of the absolute number of elderly persons infected with resistant type influenza in all epidemics (minor and major). This figure greatly resembles Figure 7.35.

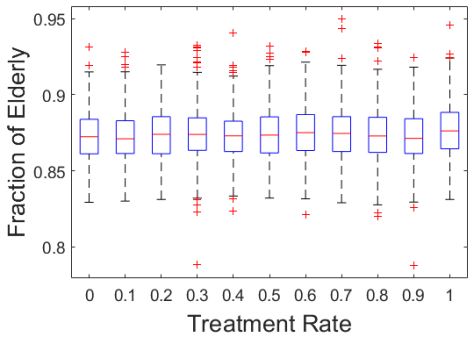

FIGURE 7.38: Box-plot of the fraction of infections in major outbreaks that is elderly of 1000 simulations for different treatment times.

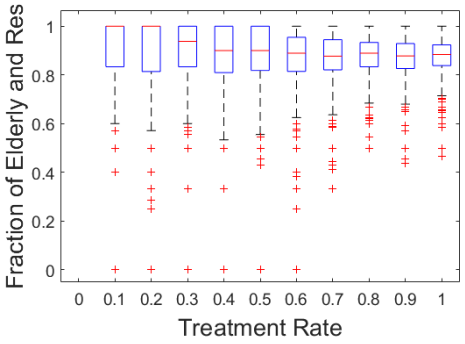

FIGURE 7.39: Box-plot of the fraction of infections in major outbreaks that is elderly and with resistant type in major outbreaks of 1000 simulations for different treatment times.

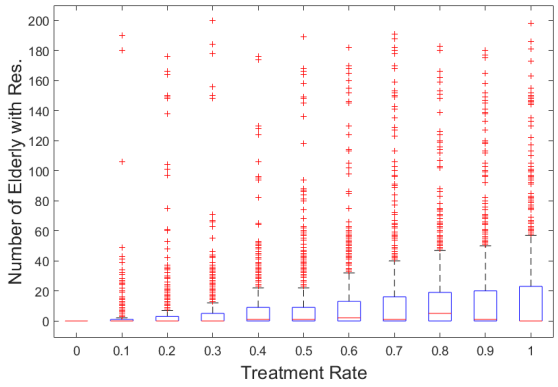

FIGURE 7.40: Box-plot of number of elderly infected with resistant type during all epidemics for all treatment rates.

Conclusion The difference in final size of major outbreaks are very small for different treatment rates, however the fraction of resistance in a major outbreak increases significantly for higher treatment rates. Therefore, the treatment rate should be kept as small as possible. Differences in the fraction of infections that is among elderly people are insignificant.

7.2.5 Different Treatment-efficacy Function

In this section, the treatment-efficacy is not constant from the moment that treatment starts. The efficacy of the treatment increases in a few steps. Treatment starts at 15 hours after infection and increases in 5 equal steps to an efficiency of 0.97 at 40 hours. The treatment rate is kept constant at 0.6. The results of 1000 simulations of this type are compared with treatment at 15 hours with perfect efficacy and a treatment rate of 0.6 per elderly that got infected.

The number of major outbreaks out of 1000 simulations is 325. This is not significantly different from the number of major outbreaks for perfect efficacy at 15 hours:

304 (p-value = 0.3119). Figure 7.41 shows the distribution of the final size of major outbreaks for both cases. These are found to be significantly different (p-value = 2.9409×10^{-4}). The mean of the final size of a major outbreak for perfect efficacy is 168.8, where the mean for the increasing efficacy is equal to 178.3.

The distributions for the fraction of infections of a major outbreak that is with resistant type are shown in Figure 7.42. They are obviously different (p-value = 3.582×10^{-116}). The reason for this can be found in Figure 7.43. The main explanation for the higher probability of the appearance of resistance is that mutation events can now take place, even when treatment is already (partly) applied. Resistant viruses that appear when treatment already started have a competitive advantage with respect to the sensitive viruses, as their production is limited. Therefore, they are more likely to spread within a host.

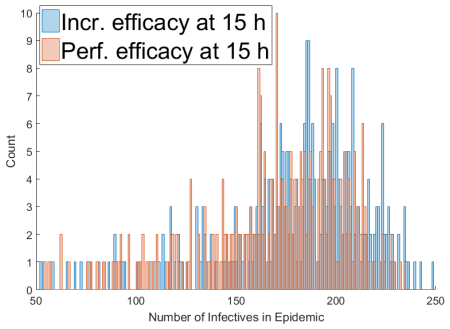

FIGURE 7.41: Histogram of final size of major outbreaks of 1000 simulations of between-host model for different treatment-efficacy functions.

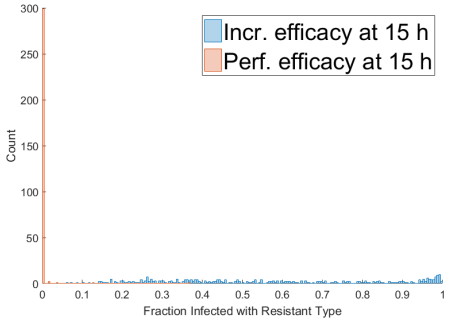

FIGURE 7.42: Histogram of fraction of resistant infections in major outbreaks of 1000 simulations of between-host model for different treatment-efficacy functions.

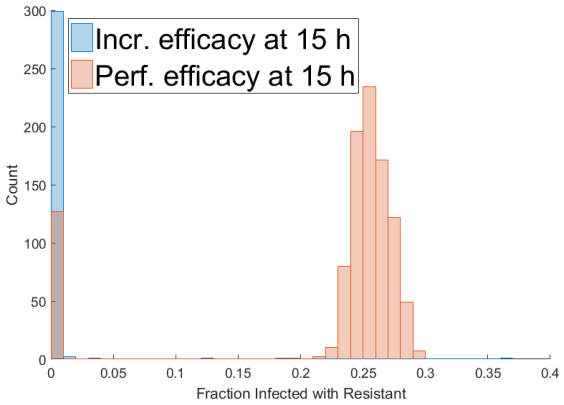

FIGURE 7.43: Histogram of fraction of cells infected with resistant type influenza in 1000 within-host simulations for different treatment-efficacy functions.

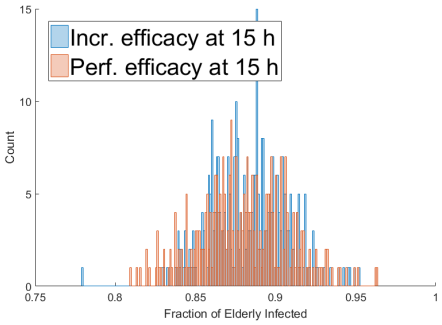

FIGURE 7.44: Histogram of fraction of infections of elderly in major outbreaks of 1000 simulations of between-host model for different treatment-efficacy functions.

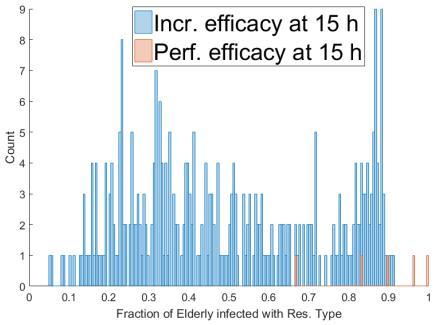

FIGURE 7.45: Histogram of fraction of infections of elderly with resistant type in major outbreaks of 1000 simulations of between-host model for different treatment-efficacy functions.

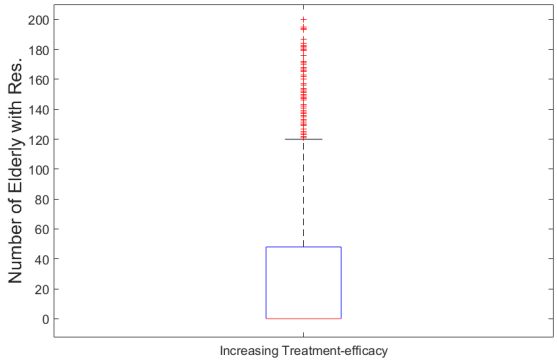

FIGURE 7.46: Box-plot of number of elderly infected with resistant type during an epidemic with an increasing treatment-efficacy function.

Figure 7.44 shows the distributions of the fraction of infections that is an elderly person for major outbreaks in both cases. These distributions are significantly different (p-value = 0.0319). The mean of the distribution for the perfect efficacy is equal to 0.8796 and for the increasing efficacy 0.8838.

The differences in the number of resistant cases that appear in both cases has a great influence on Figure 7.45 as well. This figure shows the distribution of the fraction of resistant cases that is among elderly people. The main difference is the number of observations for both. For the perfect efficacy function, only a few observations of elderly persons with resistant infections were made. This is in great contrast to the distribution for the increasing efficacy function. The distribution of the absolute number of elderly persons infected with resistant type influenza for the increasing treatment-efficacy function is shown in Figure 7.46.

Conclusion The probability for appearance of resistance is much higher for an increasing treatment-efficacy function than for perfect efficacy from the start of treatment.

Chapter 8

Sellke Construction for Between-host Model

The results of the between-host model suggest that the distribution of the final size is Gaussian, however this is not supported by statistical tests. The goal of this chapter is to find the distribution of the final size of an epidemic in the between-host model analytically. In order to do so the model is described in a different (but equivalent) way. This new description allows for an analytical expression for the final size. The technique was first used by Sellke to find the distribution of the final size of a stochastic epidemic. Diekmann and Britton described his technique clearly in their book. Their approach Diekmann and Britton is extended to be applicable for the between-host model, as it has not been used on a two-strain type model before. For the description of the between-host model recall Chapter 6. There are two possible approaches to use build a Sellke construction for this model, both are described in this chapter, but first the R_0 of the model is evaluated.

8.1 R_0 of Between-host model

The R_0 of the between host model can be found using the next generation-technique of Driessche and Watmough (2002). The next-generation matrix is divined as FV^{-1}, where F contains information about the rate of new infections and V about changes not related to new infections. A detailed description of both matrices is given in Driessche and Watmough, 2002. For the between-host model F is given by:

$$F = \begin{pmatrix} \alpha_s & (1-p)\alpha_t & 0 \\ 0 & 0 & 0 \\ 0 & p\alpha_t & \alpha_r \end{pmatrix} \tag{8.1}$$

and V by

$$V = \begin{pmatrix} \sigma + \eta_s & 0 & 0 \\ -\sigma & \eta_t & 0 \\ 0 & 0 & \eta_r. \end{pmatrix} \tag{8.2}$$

Hence, the next-generation is

$$FV^{-1} = \begin{pmatrix} \frac{\alpha_s}{\sigma+\eta_s} + \frac{\sigma(1-p)\alpha_t}{(\sigma+\eta_s)\eta_t} & \frac{(1-p)\alpha_t}{\eta_t} & 0 \\ 0 & 0 & 0 \\ \frac{\sigma p\alpha_t}{(\sigma+\eta_s)\eta_t} & \frac{p\alpha_t}{\eta_t} & \frac{\alpha_r}{\eta_r}. \end{pmatrix} \tag{8.3}$$

The next-generation techniques gives that R_0 is equal to the spectral radius of the next-generation matrix. Therefore, $R_0 = \max\{\frac{\alpha_r}{\eta_r}, \frac{\alpha_s}{\sigma+\eta_s} + \frac{\sigma(1-p)\alpha_t}{(\sigma+\eta_s)\eta_t}\}$.

8.2 Method 1 - One Infectious Pressure

Let $\{l_i\}_{i=1}^N$ be i.i.d. randomly distributed variables with density e^{-t} on $[0, \infty)$. $\{l_{(i)}\}_{i=1}^N$ is the ordered variant of $\{l_i\}_{i=1}^N$ from small to large. These define a threshold value for getting infected with (respectively) sensitive or resistant type influenza.

Furthermore, define the following equation for the infectious pressure;

$$\lambda_c(t) = \frac{\alpha_s}{N}\int_0^t I_s(x)dx + \frac{\alpha_t}{N}\int_0^t I_s^t(x)dx + \frac{\alpha_r}{N}\int_0^t I_r(x)dx. \tag{8.4}$$

The epidemic starts with 1 infective of sensitive type, which makes sure that the value of the infectious pressures becomes larger than zero. When the infectious pressure of λ_c exceeds the value of l_i person i gets infected. The infective is infected with resistant type with probability q. Note that this probability q is not equal to p of the between-host model, p is the probability that a person infected with sensitive strain under treatment infects someone with resistant type, where q is the overall probability that a new infective is infected with resistant type. If the infection is with sensitive type (which happens with probability $1-q$), it will receive treatment with probability σ. It is assumed that these three categories; resistant infection, sensitive infection and sensitive infection with treatment, are three distinct categories and they do not overlap. So in fact, the sensitive infections with treatment are a separate group and not a subgroup of the sensitive type. Already at the moment of initial infection the distinction between those three groups is made.

When the infection is with sensitive type the infectious period is choses from the an exponential distribution with mean η_s. In case of a resistant infection the distribution has mean η_r. And when treatment is applied the distribution has mean η_t. The infectious period of person i is indicated with T_i^s, T_i^r or T_i^t depending on the type of infection.

The description above is equivalent to the original description of the model when:

- the rates at which new individuals get infected are equal,
- the distributions of the infectious periods are equal.

The distributions of the infectious periods are equal by construction. Next, the rate of new infections is considered. When a new person gets infected with sensitive type, the infectious pressure increases with $\frac{\alpha_s}{N}$. Therefore the rate at which new persons get infected with sensitive type equals $\frac{\alpha_s}{N}I_s(t)S(t)$, which is equivalent to the original model. A similar reasoning holds for the rate at which new individuals get infected with resistant type or are under treatment.

However, when the new infective is sensitive the total infectious pressure is increased, not only for the sensitive type. The result is that this increases the probability that someone gets infected with resistant type as well, although there are not more infections with resistant type than before.

The above mentioned problem can be solved by correcting the probability of infecting new people with resistant type, based on the number of infections with resistant strain and sensitive time under treatment at time t. So, the probability q that someone is infected with resistant type is not constant;

$$q(t) = \frac{\frac{\alpha_t p}{N} I_s^t(t) + \frac{\alpha_r}{N} I_r(t)}{\frac{\alpha_t}{N} I_s^t(t) + \frac{\alpha_r}{N} I_r(t) + \frac{\alpha_s}{N} I_s(t)}. \tag{8.5}$$

Distribution of final size for Method 1

With this construction, it is possible to use the same arguments as Diekmann and Britton, 2012 used to find the distribution of the final size.

Let:

$$J(w) = \frac{\alpha_s}{N} \sum_{i=0}^{[w_s]-1} \Delta T_i^s + \frac{\alpha_t}{N} \sum_{i=0}^{[w_t]-1} \Delta T_i^t + \frac{\alpha_r}{N} \sum_{i=0}^{[w_r]-1} \Delta T_i^r \tag{8.6}$$

where $w = w_s + w_t + w_r$. $J(w)$ gives the total infectious pressure of the first w infectives, including the first infective with label zero. Moreover, let

$$Z(v) = \sum_{i=1}^{N} 1_{\{l_i \leq v\}}, \tag{8.7}$$

which counts the number of individuals that get infected by an infectious pressure of v.

The final size of an epidemic is reached when the current infectious pressure is not high enough to infect new individuals. Therefore, the final size can be written as;

$$Y = \min\{k \geq 0 : l_{k+1} > \frac{\alpha_s}{N} \sum_{i=0}^{k_s} \Delta T_i^s + \frac{\alpha_t}{N} \sum_{i=0}^{k_t} \Delta T_i^t + \frac{\alpha_r}{N} \sum_{i=0}^{k_r} \Delta T_i^r\}, \tag{8.8}$$

where $k = k_s + k_t + k_r$. Using the functions described above this can be rewritten as;

$$Y = \min\{w \geq 0 : Z(J(w+1)) = w\}. \tag{8.9}$$

$Z(J(w+1))$ are the number of people that get infected by the infectious pressure of the first $w+1$ infectives, so w new infectives and the initial one. If this number is equal to w, that means that the infectious pressure of the first $w+1$ infectives is exactly enough to infect w initial susceptibles and not more. The final size of the epidemic is thus equal to w.

The main reason to write the final size as done in Equation 8.9 is that the final size is now the intersection of a composition of two independent processes and a straight line (w). Now the techniques of Diekmann and Britton, 2012 can be used without adjustments to conclude that the final size of the epidemic will converge to the smallest non-negative solution of;

$$1 - e^{-(\frac{\alpha_s}{N} E(\Delta T^s) + \frac{\alpha_t}{N} E(\Delta T^t) + \frac{\alpha_r}{N} E(\Delta T^r))x} = x. \tag{8.10}$$

And it is also found that the distribution around this limit is Gaussian as N goes to infinity.

8.3 Method 2 - Two Infectious Pressures

Let $\{l_i^s\}_{i=1}^N$ and $\{l_i^r\}_{i=1}^N$ be i.i.d. randomly distributed variables with density e^{-t} on $[0, \infty)$. Moreover, let $\{L_i\}_{i=1}^N := \{(l_i^s, l_i^r\}_{i=1}^N$. These define a threshold value for getting infected with respectively sensitive or resistant type influenza.

Furthermore, define the following equation for the infectious pressure due to respectively sensitive and resistant type;

$$\lambda_c^s(t) = \frac{\alpha_s}{N} \int_0^t I_s(x)dx + \frac{\alpha_t(1-p)}{N} \int_0^t I_s^t(x)dx, \tag{8.11}$$

$$\lambda_c^r(t) = \frac{\alpha_t p}{N} \int_0^t I_s^t(x)dx + \frac{\alpha_r}{N} \int_0^t I_r(x)dx. \tag{8.12}$$

The epidemic starts with one infective with sensitive type infection. Therefore, the value of the infectious pressure for the sensitive type becomes positive. When the infectious pressure of λ^s exceeds the value of l_i^s, person i gets infected with sensitive type. Treatment is applied to each new infective with probability σ. Hence, the infectious pressure of the resistant strain becomes larger than zero as well. When the value of λ_c^r gets larger than l_i^r for some i, that person will suffer from an infection with resistant type influenza.

Again, when the infection is with sensitive type the infectious period is chosen from an exponential distribution with mean η_s. In the case of a resistant infection the distribution has mean η_r. When treatment is applied the distribution has mean η_t. The infectious period of person i is indicated with T_i^s, T_i^r or T_i^t depending on the type of infection.

As before, the distributions of the infectious periods are equivalent to the original description of the model. However, the rates of getting new infectives also have to be equivalent. This is clearly the case, as having one infective with sensitive type increases the pressure of getting new sensitive infectives with $\frac{\alpha_s}{N}$ and infectives under treatment with $\frac{\alpha_t(1-p)}{N}$ for sensitive type and $\frac{\alpha_t p}{N}$ for the resistant type. A new infection with resistant type increases the infectious pressure for new resistant infections with $\frac{\alpha_r}{N}$. These are similar to the rates of new infections in the original model. Therefore, both descriptions are equivalent for the model.

Distribution of Final Size for Method 2

Similar techniques as for the first method will be used here. However, in this description persons could get infected with both types of virus. As for each person there are two different threshold values, it is not possible to order the thresholds. Therefore, it is not possible to remove a person from the susceptible group for the other type after infection with one type. The following analysis allows thus for double infections.

Let;

$$J^s(w_s) = \frac{\alpha_s}{N} \sum_{i=0}^{[w_s]-1} \Delta T_i^s + \frac{\alpha_t(1-p)}{N} \sum_{i=0}^{[w_t]-1} \Delta T_i^t, \tag{8.13}$$

$$J^r(w_r) = \frac{\alpha_t(p)}{N} \sum_{i=0}^{[w_t]-1} \Delta T_i^t + \frac{\alpha_r}{N} \sum_{i=0}^{[w_r]-1} \Delta T_i^r. \tag{8.14}$$

$J(w_s)$ and $J(w_s)$ give the total infectious pressure of the first w infectives for respectively sensitive and resistant type, including the initially infective with label zero. Moreover, let

$$Z^s(v) = \sum_{i=1}^{N} 1_{\{l_i^s \leq v\}}, \tag{8.15}$$

$$Z^r(v) = \sum_{i=1}^{N} 1_{\{l_i^r \leq v\}}, \tag{8.16}$$

give the number of people infected with either sensitive of resistant type if the infectious pressure is equal to v.

The technique of Diekmann and Britton, 2012 gives that the number of people infected with sensitive and resistant type have limits which are the smallest non-negative solutions of;

$$1 - e^{(\frac{\alpha_s}{N} E(\Delta T^s) + \frac{\alpha_t(1-p)}{N} E(\Delta T^t))x_s} = x_s, \tag{8.17}$$

$$1 - e^{(\frac{\alpha_t p}{N} E(\Delta T^t) + \frac{\alpha_r}{N} E(\Delta T_i^r))x_r} = x_r. \tag{8.18}$$

Moreover, it can be proven with the central limit theorem, that the distribution around the limit is Gaussian again. However, this is only true when double infections are allowed.

Conclusion and Further Work

It can be concluded of the final size of the complete epidemic and its distribution are known. However, it is not clear what the limit and distribution of the number of resistant infections is. To find an expression for this either q has to be used over time in the first method or the problem with the double infection of the second method has to be solved. For now, this is left as a recommendation for future work.

Chapter 9

Discussion

9.1 Within-host

As mentioned in Section 4.3.2, mutation events cannot take place after the start of treatment. This is not corresponding with reality, as with an efficiency of 0.97, reactions still take place and there is a probability that they produce resistant viruses. However, this would be difficult to model, as the probability that resistance will occur goes to one when time goes to infinity. Note, this will only happen when treatment starts at a time when still a reasonable amount of healthy cells are available. In reality the immune response kills all viruses some time after the start of the reaction, however, in the model the number of immune cells is bounded from above. Therefore, some resistant cells could still escape the immune response in this model. The assumption that mutations do not take place after the start of the treatment does not do harm to the model. Section 4.4 confirms this, as the full Gillespie method does not include this assumptions and the results thereof are very similar to the hybrid simulation method.

Another challenge for the within-host model is to choose realistic parameters for the model. These can not be used directly from literature, as explained in 4.2. However, for investigating the appearance and spread of resistant type influenza, the relative differences in the parameters of both types are of higher importance than the absolute values. Both types will compete with each other to infect the healthy cells that are still available. The winner of such a competition only depends on the relative differences.

The mutation rate is fixed at one constant in the model, however it is not only one mutation that results in resistance. In reality, a combination of mutations is necessary (Khodadad et al., 2015). To correct for this the mutation rate used in this model is smaller than the general mutation rate of a virus. Although this might be true, this rate is not (yet) validated with experiments. Moreover, it does not incorporate the possibility that only a part of the necessary mutations take place. On the contrary, there is evidence that the mutations are linked together and that they often appear at the same time (Khodadad et al., 2015).

The choice of the switching level influences the results of the within-host level, see Section 4.4. For the smaller version of the model, that is used to compare the hybrid simulation method to a full Gillespie method, the effects of a different level could be tested, however for the larger model, this is not possible. It would be good to test the chosen switching level by comparing the results with a full Gillespie result, even though this would cost some computation time.

The same is true for the reaction rate of the empty reaction, this is picked based on the results of the smaller model. However, a comparison with a full Gillespie simulation set of the full model could determine the best choice of this parameter.

9.2 Linking both scales

It is not known how transmission takes place. There are two routes in general; direct contact (DC) and respiratory droplets (RD). Resistant strain can not be spread by DC, however sensitive strain can (Frise et al., 2016). In the model it is assumed that the difference in spread between resistant and sensitive type is only caused by difference in infectious load. Hence, the difference in the probability to spread between resistant and sensitive type could be even larger.

Another factor of uncertainty is how many viruses are needed to infect one person. There exists proof that one virus is enough (Frise et al., 2016). However, in the simplified within-host model, the number of infected cells is used as input, not the number of viruses. During the simulations each infection starts with 100 infected cells from one of the two types. The choice to start with 100 cells instead of 1 is made to eliminate the probability that an infection does not take off. However, the probability that if one cell in a host is infected then at least 100 cells get infected is 0.99. This probability is measured with 1000 simulations of the within-host model, where the initial condition was only one infected cell.

In reality, a person that gets infected by, for instance, breathing in an aerosol that contains viruses from a patient under treatment will get infected with both types of viruses at the same time. This possibility is however not modeled.

9.3 Between-host

The contact matrix that is used for modeling the spread of resistance in the between-host model is not based on research and is therefore chosen arbitrarily. It would be good to have data on how HCWs and elderly interact with each other, in order to improve this part of the model.

9.4 Future Work

The complete model could be used to compare more different strategies to prevent the spread of resistance. For instance, more complex vaccinating strategies or more variants of the treatment-efficacy function. Moreover, the effect of the mutation rate on the appearance and spread of drug-resistant influenza could be evaluated.

Moreover, a quantitative way to compare different strategies is useful in order to make recommendations for new policies in old people's homes. This could be done by calculating cost of an epidemic as a function of the number of elderly people that get infected, the number of resistant infections and the number of elderly people infected with resistant type influenza.

It has been shown that the efficacy function of the treatment has great influence on the appearance and spread of the drug-resistant strain. However, it is not yet known how the efficacy of the treatment looks in reality. This information could improve the results of the modeling.

Finally, the analysis of the distribution of the final size in Chapter 8 can be continued. For instance, to find the distribution of the final size of the number of resistant infections during an epidemic.

Appendix A

Additional Results

A.1 Compare Within-host Model with Deterministic Solution

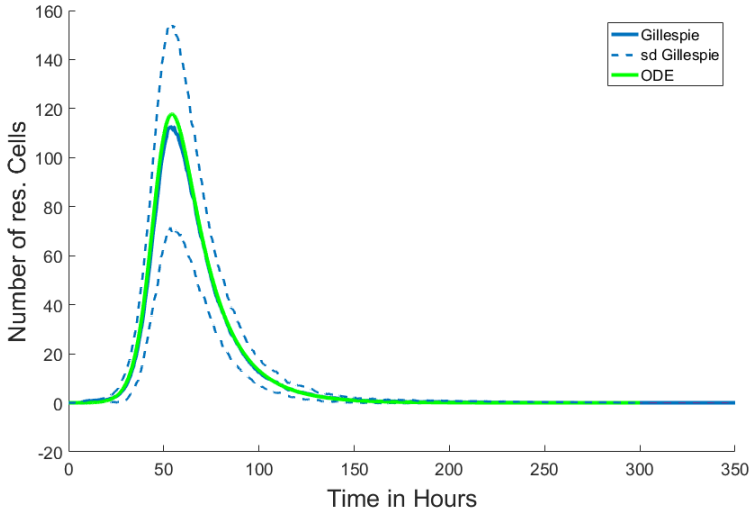

FIGURE A.1: Mean of 300 simulations of a full Gillespie approach (solid blue line) and deterministic solution of within-host model without treatment. Dashed lines indicate one standard deviation away from the mean.

A.2 Between Host Model

The results of the comparisons of the number of final outbreaks and of the distributions of results from the between host model are summarized in this Appendix. A p-value of 0 in a table means that the p-value smaller is than 10^{-10}. N.d. stands for no data and indicates that none of the simulations resulted in an observation for one of the categories that are compared.

Initial Infective

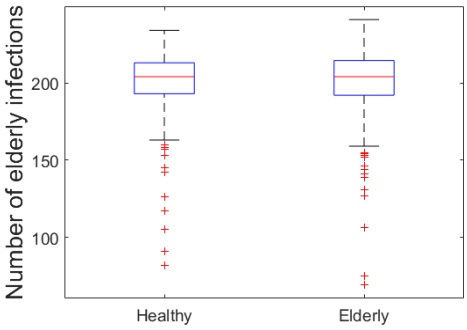

FIGURE A.2: Box-plot of number of elderly people infected in major outbreaks where the initial infective is either a HCW or an elderly.

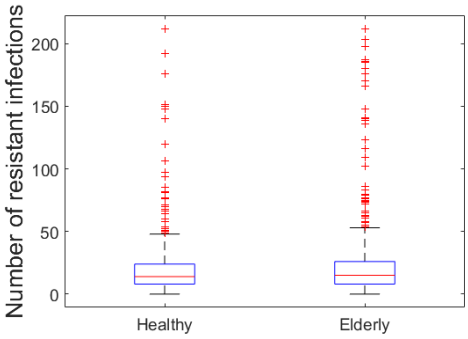

FIGURE A.3: Box-plot of number of resistant infections in major outbreaks where the initial infective is either a HCW or an elderly.

Vaccinating

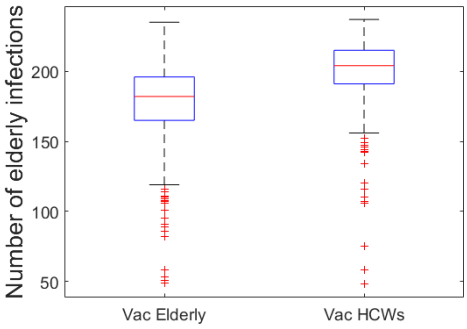

FIGURE A.4: Box-plot of number of elderly infected in major outbreaks for vaccinating the elderly or the HCWs.

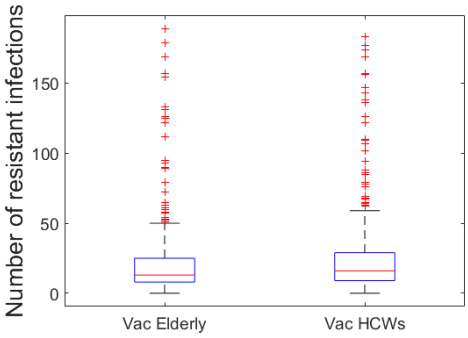

FIGURE A.5: Box-plot of number of resistant infections in major outbreaks for vaccinating the elderly or the HCWs.

Treatment Timing

TABLE A.1: P-values for testing the differences between the number of major outbreaks for different treatment times.

Treatment Time (hours)	15	20	25	30	35	40	45
15	1	$1.421\ 10^{-7}$	0	0	0	0	0
20	-	1	0.0061	0.0426	0.0002	0.0012	0.0001
25	-	-	1	0.4735	0.3036	0.6226	0.2635
30	-	-	-	1	0.0809	0.2267	0.0666
35	-	-	-	-	1	0.5914	0.9287
40	-	-	-	-	-	1	0.5312
45	-	-	-	-	-	-	1

TABLE A.2: Means and medians of the distribution of the final sizes of major outbreaks and fraction of resistance in major outbreaks for different treatment times.

	Mean Final Size	Median Final Size	Mean Fraction Resistant	Median Fraction Resistant
15	168.80	174	0.0019	0
20	205.99	210	0.0229	0
25	226.26	230	0.0578	0.0238
30	225.06	231	0.1969	0.1345
35	236.43	237	0.0002	0
40	236.06	239	$5.733\ 10^{-5}$	0
45	236.47	238	0	0

TABLE A.3: P-values of Mann-Whitney U test for distribution of final size of major outbreaks of all combinations of treatment times.

Treatment Time (hours)	15	20	25	30	35	40	45
15	1	0	0	0	0	0	0
20	-	1	0	0	0	0	0
25	-	-	1	0.8027	0	0	0
30	-	-	-	1	0	0	0
35	-	-	-		1	0.9333	0.6858
40	-	-	-	-	-	1	0.7918
45	-	-	-	-	-	-	1

TABLE A.4: P-value of Mann-Whitney U test for distribution of fraction of infections that is with resistant strain in major outbreaks for different treatment times. NaN appears because all values are zero for treatment time at 45 hours.

Treatment Time (hours)	15	20	25	30	35	40	45
15	1	0	0	0	0.9395	0.0230	0.0039
20	-	1	0	0	0	0	0
25	-	-	1	0	0	0	0
30	-	-	-	1	0	0	0
35	-	-	-	-	1	0.0214	0.0045
40	-	-	-	-	-	1	0.3114
45	-	-	-	-	-	-	NaN

TABLE A.5: Means and medians for distribution of the fraction of the infections in a major outbreak that is elderly and the fraction of the resistant infections in a major outbreak that is elderly for different treatment times. NaN indicates that there were no observations of elderly infected with resistant type.

	Mean Fraction Elderly	Median Fraction Elderly	Mean Fraction Resistant and Elderly	Median Fraction Resistant and Elderly
15	0.8796	0.8790	NaN	NaN
20	0.8777	0.8774	NaN	NaN
25	0.8751	0.8740	NaN	NaN
30	0.8747	0.8735	0.8774	0.8850
35	0.8729	0.8717	NaN	NaN
40	0.8733	0.8734	NaN	NaN
45	0.8725	0.8714	NaN	NaN

TABLE A.6: P-values of Mann-Whitney U test of distribution of fraction of infections that is elderly in a major outbreak for different treatment times.

Treatment Time (hours)	15	20	25	30	35	40	45
15	1	0.2857	0.0167	0.0068	0.0001	0.0005	0
20	-	1	0.1106	0.0499	0.0004	0.0038	0.0003
25	-	-	1	0.5743	0.0234	0.1521	0.0179
30	-	-	-	1	0.1144	0.4136	0.0831
35	-	-	-		1	0.4238	0.9253
40	-	-	-	-	-	1	0.3734
45	-	-	-	-	-	-	1

TABLE A.7: P-values of Mann-Whitney U test of distribution of fraction of resistant infections that is elderly in a major outbreak for different treatment times. N.d. (no data) indicates that there were no people infected with resistant strain in all simulations of one type and therefore all fractions were $\frac{0}{0} = NaN$ and the statistical test could not be performed.

Treatment Time (hours)	15	20	25	30	35	40	45
15	1	0.1811	0.5798	0.7846	0.2704	0.6667	n.d.
20	-	1	0.0066	0	0.6416	0.4534	n.d.
25	-	-	1	$1.900\ 10^{-6}$	0.3050	0.3235	n.d.
30	-	-	-	1	0.0292	0.1092	n.d.
35	-	-	-	-	1	1	n.d.
40	-	-	-	-	-	1	n.d.
45	-	-	-	-	-	-	n.d.

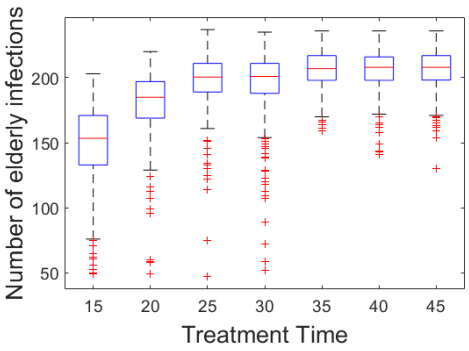

FIGURE A.6: Box-plots for the number of elderly people infected during a major outbreak for different treatment times.

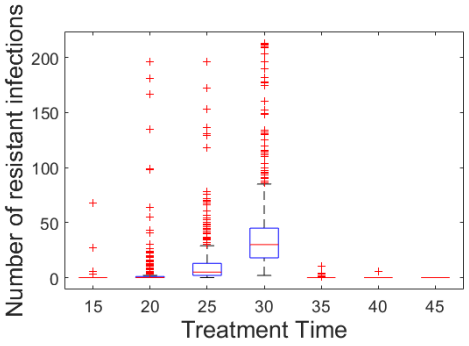

FIGURE A.7: Box-plots for the number of resistant infections during a major outbreak for different treatment times.

Treatment Rates

TABLE A.8: P-values of testing the difference between the number of major outbreaks for different treatment rates.

	0	0.1	0.2	0.3	0.4	0.5	0.6	0.7	0.8	0.9	1
0	1	0.3475	0.8933	0.5610	0.7205	0.9643	0.6547	0.3710	0.4208	0.3035	0.1072
0.1	-	1	0.4207	0.1284	0.5608	0.3710	0.6226	0.0667	0.8932	0.0491	0.0108
0.2	-	-	1	0.4743	0.8231	0.9287	0.7542	0.3036	0.5022	0.2448	0.0810
0.3	-	-	-	1	0.3476	0.5312	0.3037	0.7541	0.1656	0.6545	0.3031
0.4	-	-	-	-	1	0.7542	0.9287	0.2105	0.6546	0.1656	0.0490
0.5	-	-	-	-	-	1	0.6873	0.3476	0.4470	0.2830	0.0978
0.6	-	-	-	-	-	-	1	0.1797	0.7204	0.1310	0.0396
0.7	-	-	-	-	-	-	-	1	0.0892	0.8932	0.4736
0.8	-	-	-	-	-	-	-	-	1	0.0667	0.0157
0.9	-	-	-	-	-	-	-	-	-	1	0.5603
1	-	-	-	-	-	-	-	-	-	-	1

TABLE A.9: The mean and median values of the distribution of the final size of major outbreaks and the fraction of resistance in major outbreaks for different treatment rates.

	Mean Final Size	Median Final Size	Mean Fraction Resistant	Median Fraction Resistant
0	237.40	239	0	0
0.1	235.54	238	0.0195	0.0042
0.2	233.26	237	0.0461	0.0159
0.3	233.31	235	0.0550	0.0255
0.4	231.50	236	0.0746	0.0445
0.5	230.13	234	0.0951	0.0478
0.6	228.65	232	0.1105	0.0649
0.7	229.39	233	0.1456	0.0822
0.8	228.36	232	0.1474	0.0913
0.9	227.08	233	0.1707	0.1097
1	226.22	231	0.1964	0.1220

TABLE A.10: P-values of Mann-Whitney U test for final size of major outbreaks of 1000 simulations of different treatment rates.

	0	0.1	0.2	0.3	0.4	0.5	0.6	0.7	0.8	0.9	1
0	1	0.1758	0.0042	0.0008	0.0004	$3.276\ 10^{-6}$	0	$9.944\ 10^{-8}$	$4.861\ 10^{-10}$	$9.506\ 10^{-9}$	0
0.1	-	1	0.1302	0.0475	0.0246	0.0008	$2.360\ 10^{-7}$	$5.064\ 10^{-5}$	$9.076\ 10^{-7}$	$5.050\ 10^{-6}$	$4.792\ 10^{-9}$
0.2	-	-	1	0.6542	0.4377	0.0676	0.0003	0.0109	0.0008	0.0022	$1.620\ 10^{-5}$
0.3	-	-	-	1	0.7301	0.1619	0.0011	0.0281	0.0027	0.0075	$6.211\ 10^{-5}$
0.4	-	-	-	-	1	0.3107	0.0069	0.0868	0.0123	0.0259	0.0005
0.5	-	-	-	-	-	1	0.0885	0.4468	0.1325	0.1874	0.0106
0.6	-	-	-	-	-	-	1	0.3569	0.8776	0.7775	0.3220
0.7	-	-	-	-	-	-	-	1	0.4478	0.5513	0.0692
0.8	-	-	-	-	-	-	-	-	1	0.9107	0.2782
0.9	-	-	-	-	-	-	-	-	-	1	0.2363
1	-	-	-	-	-	-	-	-	-	-	1

TABLE A.11: P-values of testing the difference between the distributions of the fraction of the infections in a major outbreak that is with resistant type for different treatment rates.

	0	0.1	0.2	0.3	0.4	0.5	0.6	0.7	0.8	0.9	1
0	NaN	0	0	0	0	0	0	0	0	0	0
0.1	-	1	0	0	0	0	0	0	0	0	0
0.2	-	-	1	$4.614\ 10^{-8}$	0	0	0	0	0	0	0
0.3	-	-	-	1	0	0	0	0	0	0	0
0.4	-	-	-	-	1	0.0322	0	0	0	0	0
0.5	-	-	-	-	-	1	$4.645\ 10^{-7}$	0	0	0	0
0.6	-	-	-	-	-	-	1	$1.034\ 10^{-5}$	0	0	0
0.7	-	-	-	-	-	-	-	1	0.0267	$2.147\ 10^{-6}$	0
0.8	-	-	-	-	-	-	-	-	1	0.0059	$4.808\ 10^{-9}$
0.9	-	-	-	-	-	-	-	-	-	1	0.0026
1	-	-	-	-	-	-	-	-	-	-	1

TABLE A.12: Means and medians for distribution of the fraction of the infections in a major outbreak that is elderly and the fraction of the resistant infections in a major outbreak that is elderly for different treatment rates. NaN indicates that there were no observations of elderly infected with resistant type.

	Mean Fraction Elderly	Median Fraction Elderly	Mean Fraction Resistant and Elderly	Median Fraction Resistant and Elderly
0	0.87210	0.8723	NaN	NaN
0.1	0.8722	0.8710	NaN	NaN
0.2	0.8738	0.8739	NaN	NaN
0.3	0.8746	0.8739	NaN	NaN
0.4	0.8732	0.8729	NaN	NaN
0.5	0.8738	0.8734	NaN	NaN
0.6	0.8750	0.8750	NaN	NaN
0.7	0.8746	0.8745	NaN	NaN
0.8	0.8738	0.8729	0.8764	0.8889
0.9	0.8725	0.8712	0.8730	0.8778
1	0.8770	0.8762	0.8727	0.8836

TABLE A.13: P-values for testing differences in the distribution of the fraction of elderly infected in a major outbreak with Mann-Whitney U test.

	0	0.1	0.2	0.3	0.4	0.5	0.6	0.7	0.8	0.9	1
0	1	0.4699	0.3199	0.1156	0.6411	0.4224	0.0304	0.1348	0.3437	0.8184	0.0003
0.1	-	1	0.0680	0.0187	0.1917	0.1232	0.0029	0.0231	0.0895	0.6814	$1.703\ 10^{-5}$
0.2	-	-	1	0.6503	0.5097	0.8292	0.2762	0.6452	0.8957	0.2072	0.0124
0.3	-	-	-	1	0.2601	0.4995	0.5144	0.9704	0.5395	0.0738	0.0357
0.4	-	-	-	-	1	0.6708	0.0713	0.2679	0.6105	0.4718	0.0012
0.5	-	-	-	-	-	1	0.2030	0.5105	0.9159	0.2971	0.0066
0.6	-	-	-	-	-	-	1	0.5211	0.2095	0.0190	0.1354
0.7	-	-	-	-	-	-	-	1	0.5612	0.0916	0.0377
0.8	-	-	-	-	-	-	-	-	1	0.2524	0.0075
0.9	-	-	-	-	-	-	-	-	-	1	0.0003
1	-	-	-	-	-	-	-	-	-	-	1

TABLE A.14: P-values of Mann-Whitney U test of distribution of fraction of resistant infections that is elderly in a major outbreak for different treatment rates. N.d. (no data) indicates that there were no people infected with resistant strain in all simulations of one type and therefore all fractions were $\frac{0}{0} = NaN$ and the statistical test could not be performed.

	0	0.1	0.2	0.3	0.4	0.5	0.6	0.7	0.8	0.9	1
0	-	n.d.	n.d.	n.d.	n.d.	n.d.	n.d.	n.d.	n.d.	n.d.	n.d.
0.1	-	1	0.2036	0.0090	n.d.	n.d.	n.d.	n.d.	n.d.	n.d.	n.d.
0.2	-	-	1	0.1635	n.d.	n.d.	n.d.	n.d.	n.d.	n.d.	n.d.
0.3	-	-	-	1	n.d.	n.d.	n.d.	n.d.	n.d.	n.d.	n.d.
0.4	-	-	-	-	n.d.	n.d.	n.d.	n.d.	n.d.	n.d.	n.d.
0.5	-	-	-	-	-	n.d.	n.d.	n.d.	n.d.	n.d.	n.d.
0.6	-	-	-	-	-	-	n.d.	n.d.	n.d.	n.d.	n.d.
0.7	-	-	-	-	-	-	-	n.d.	n.d.	n.d.	n.d.
0.8	-	-	-	-	-	-	-	-	n.d.	n.d.	n.d.
0.9	-	-	-	-	-	-	-	-	-	n.d.	n.d.
1	-	-	-	-	-	-	-	-	-	-	n.d.

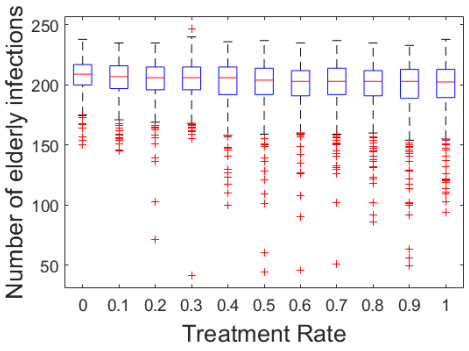

FIGURE A.8: Box-plot of the number of elderly people that got infected during a major outbreak for 1000 simulations for each treatment rate.

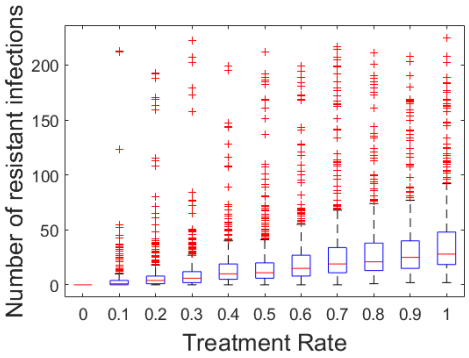

FIGURE A.9: Box-plot of the number of resistant infections during a major outbreak for 1000 simulations for each treatment rate.

Treatment Efficiency

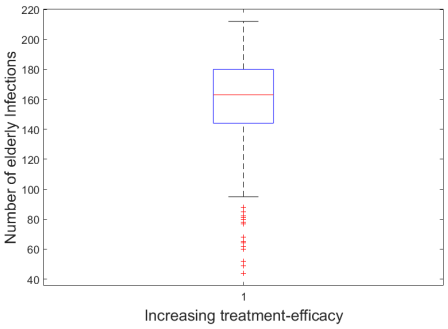

FIGURE A.10: Box-plot of the number of elderly people that got infected during a major outbreak for 1000 simulations for the increasing treatment-efficacy function.

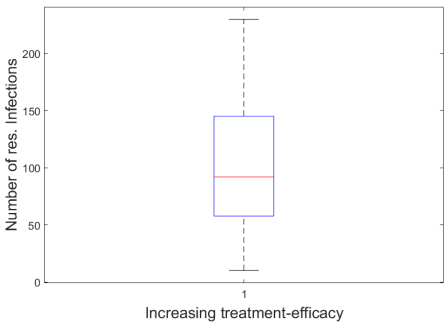

FIGURE A.11: Box-plot of the number of resistant infections during a major outbreak for 1000 simulations for the increasing treatment-efficacy function.

Appendix B

Matlab Code

B.1 Code for within host model

For simulating the within host model, two main functions are used; *treatment* and *stoch-det*. Both functions are printed in this Appendix. *Treatment* estimates the number and timing of the mutation events and gives them as an input to *stoch-det*. *Treatment* calculates these events and their timing separately for the time before and the time after treatment. *Stoch-det* uses the input from *treatment* to do the Gillespie part of the hybrid simulation model and the fast part after the switching level is reached. This is done separately for the time before and after treatment as well. Both parts are glued together in *treatment*.

In both before mentioned functions the system of fast equations and the full model of equations are used at several places, these functions are shown below as well. Moreover, the function that calculates the propensities for the slow part of the model is shown.

```
function dy = fast_treatment(t,y,treatment_eff)
% Model of the fast part including the treatment and also an
    immune response

%% set rates of system
W = 0.00001;
r = 0.0000025;
beta_s = 3.1*10^(-10);
beta_r = 2.4*10^(-10);
lambda_s = 1/6.9*0.3;
lambda_r = 1/10.5*0.3;
a_s = 1/28*1.5;
a_r = 1/11*1.5;
cs = 0.093*1.2;
cr = 0.099*1.2;
k_s = 6;
k_r = 17.5;

A = (beta_s * k_s * (1- treatment_eff) *(1 - 10^(-8)))/cs;
D = lambda_s;
E = a_s;

% system of ODE's for the generating function,
% to use in ODE45
```

```
dy = [-A*y(1)*y(3);
      A*y(1)*y(3)-D*y(2) ;
      D*y(2)-E*y(3)-W*y(3)*y(4);
      r*y(4)*(20000-y(4))];
end
```

```
function dy = full_model(t,y,treatment_eff)
% FUll ODE model of the within host part.

%% set rates of system
W = 0.000015;
r = 0.0000025;
beta_s = 3.1*10^(-10);
beta_r = 2.4*10^(-10);
lambda_s = 1/6.9*0.3;
lambda_r = 1/10.5*0.3;
a_s = 1/28*1.5;
a_r = 1/11*1.5;
cs = 0.093*1.2;
cr = 0.099*1.2;
k_s = 6;
k_r = 17.5;

A = (beta_s * k_s * (1- treatment_eff) *(1 - 10^(-8)))/cs;
B = (beta_r*k_r)/cr;
D = lambda_s;
E = a_s;
F = lambda_r;
G = a_r;

% system of ODE's for the generating function,
% to use in ODE45
    dy = [-A*y(1)*y(3)-B*y(1)*y(6); % mutatie hoeft hier niet
        meer in, omdat of alle mutaties al geweest zijn?!
          A*y(1)*y(3)-D*y(2);
          D*y(2)-E*y(3) - W*y(4)*y(3);
          r*y(4)*(20000-y(4));
          B*y(1)*y(6) - F*y(5);
          F*y(5) - G*y(6) - W *y(4)*y(6)];

end
```

```
function a = propensities_slow(x,xslow)
% Returns reaction propensities for the slow part of the
    model given current state x

X  = x(1);
u = x(2);
lr = xslow(1);
yr = xslow(2);

```

```
beta_s = 3.1*10^(-10);
beta_r = 2.4*10^(-10);
lambda_s = 1/6.9*0.3;
lambda_r = 1/10.5*0.3;
a_s = 1/28*1.5;
a_r = 1/11*1.5;
cs = 0.093*1.2;
cr = 0.099*1.2;
k_s = 6;
k_r = 17.5;

B = (beta_r*k_r)/cr;
F = lambda_r;
G = a_r;
r = 0.000004;

a = [B*X*yr;
     F*lr;
     G*yr;
     r*u*yr;
     90];

end
```

```

function [t_fast, x_fast_out, t_slow, x_slow_out] = treatment
   (treatment_time, treatment_eff, t_end_sim, fit, init)
 % treatment evaluates the full within host model where
    treatment starts at
 % time treatment_time and the efficiency of the treatment is
    treatment_eff,
 % the simulation ends at t_end_sim. If a person is old fit =
    0 and if a
 % person is young fit = 1

 % if fit = 1, the immune response works well
if fit
    X0 = [4*10^8,init(1),0,1000,init(2),0];
else
    X0 = [4*10^8,init(1),0,1,init(2),0];
end

 % finding points of immigration
mu = 10^(-8);

options = odeset('RelTol',1e-12,'AbsTol',1e-12);
sol1 = ode15s(@(t,y) fast_treatment(t,y,0),[0 treatment_time
   ],X0(1:4),options);

 % in this part the mutation of newly resistant virions is
    estimated
```

```
22
23  % a^s_10 estimate of the propensity
24
25  as10 = round(sol1.y(1,:)).*round(sol1.y(3,:)); % only have
        as10 for specific values of t...
26
27  as10_prob = as10/trapz(sol1.x,as10);
28
29  figure()
30  plot(sol1.x,as10_prob)
31
32  % find times at which immigration is not zero
33  times_asnz = sol1.x(as10>0);
34
35  % estimate time of one immigration reaction to take place
36  tmin=1/3600;          % resolution of one second
37  if isempty(times_asnz)
38      t_test = [];
39  else
40      tstart = times_asnz(1);
41      tend = times_asnz(end);
42
43      % make a time vector, such that on most times maximal
            number of immigrations
44      % happening is one.
45      t_test = tstart:tmin:tend;
46  end
47
48  % make new as10 based on found times
49  if isempty(t_test(t_test<treatment_time))
50      x_t1 = [];
51  else
52      x_t1 = deval(sol1,t_test(t_test<treatment_time));
53  end
54
55  if isempty(t_test(t_test>treatment_time))
56      x_t2 = [];
57  else
58      x_t2 = deval(sol2,t_test(t_test>treatment_time));
59  end
60
61  x_t = [x_t1 x_t2];
62
63  if isempty(x_t)
64      immi = [];
65  else
66      a = round(x_t(1,:)).*round(x_t(3,:));
67      % set times
68      % final time of stochastic simulation if number of
            healthy cells=zero
69      chi = floor(x_t(1,:));
```

```
    chi_zero = t_test(chi==0);
    if isempty(chi_zero)
        t_zero = tend;
    else
        t_zero = chi_zero(1);
    end

    % calculate number of reaction 10 took place
    if x_t(1,end)==0
        N = 4*10^8;
    else
        N = 4*10^8 - x_t(1,end);
    end

    % estimate number of mutation events
    if N == 0
        immi = [];
    else
        R = poissrnd(N*mu);

        % estimated times of arrival of the new resistantly
            infected cells.
        q = sort(randsample(length(t_test),R,true,a));

        immi = t_test(q);
    end
end

% model the first part, where treatment is not yet involved
[t_s_b,x_s_b,t_f_b,x_f_b] = stoch_det(0,treatment_time, X0,
    0, 1*10^3, immi);

% now introduce treatment and model from there, with starting
    values = end
% of part without treatment.
X0 = [x_f_b(end,:) x_s_b(end,:)];

[t_s_a,x_s_a,t_f_a,x_f_a] = stoch_det(treatment_time,
    t_end_sim, X0, treatment_eff, 1*10^3, immi);

% produce output
t_slow = [t_s_b; t_s_a];
x_slow_out = [x_s_b; x_s_a];

t_fast = [t_f_b  t_f_a];
x_fast_out = [x_f_b; x_f_a];

end
```

```
function [t_s,x_s,t_f,x_f] = stoch_det(t0,tlast, X0,
    treatment_eff, level, immi)
```

```
2
3  % Evaluates the model starting at time t0 until tlast using X0 at time
4  % t0, with treatment_eff as the treatment efficiency during the time
5  % peroid and I_cnt the number of immigrations that took place before t0
6  % and level is the switching level between stochastic and deterministic.
7
8      % initial conditions
9      maxn = 10000;
10
11     options = odeset('RelTol',1e-12,'AbsTol',1e-12);
12     sol = ode15s(@(t,y) fast_treatment(t,y,treatment_eff), [t0 tlast+10], X0(1:4), options);
13
14     % stoichiometry of the system
15
16     stoich_slow = [1  0;
17                   -1  1;
18                    0 -1;
19                    0 -1;
20                    0  0];
21
22         % Now, start stochastic simulation of the resistants, they now only depend
23         % on the number of healthy cells at time t
24
25         % initialization
26         xslow = zeros(maxn,2);
27         if sum(X0(5:6))==0
28             xslow(1,:) = [1  0];
29         else
30             xslow(1,:) = X0(5:6);
31         end
32
33         tSAVE = zeros(maxn,1);
34         n = 1;
35
36         % find times of mutation events
37
38         times_I = immi(immi>t0);
39         times_I = times_I(times_I<tlast);
40
41         if isempty(times_I)
42             if sum(X0(5:6))==0
43                 Q =1;
44             else
45                 t = t0;
46                 Q = 0;
```

```
47              end
48
49          else
50
51              %start at times_I(1)
52              t = times_I(1);
53
54              % remove first occurence from the list, as we
                    already put that one in
55              % xslow(1)
56              times_I(1) = [];
57
58              % switch to deterministic solving if treshold
                    level is reached or
59              % number of healthy cells has became 0.
60
61              Q = 0;
62          end
63
64          while Q==0 && xslow(n,2)<level && t<tlast  % t<
                t_final &&
65
66              %save current time t
67              tSAVE(n) = t;
68
69              X = round(deval(sol,t));
70
71              % find propensities of the reactions
72
73              a = propensities_slow([X(1) X(4)],xslow(n,:));
74              if a(1)<0
75                  a(1) = 0;
76              end
77
78              a0 = sum(a);
79
80              r = rand(1,2);
81
82              % next time step is minimum of the exected next
                    reaction of the slow
83              % process and the next immigration point. UPDATE
                    t
84
85              t_old = t;
86              t = t - log(r(1))/a0;
87
88              % Sample identity of earliest reaction channel to
                     fire (mu)
89              [~, w] = histc(r(2)*a0, [0;cumsum(a(:))]);
90
91              % Update xslow with reaction that took place
```

```
92              if w<6
93
94                  % find immigrations during the time of the
                        new reaction
95                  new_I = times_I(times_I<=t);
96
97                  % update with the new reaction
98                  xslow(n+1,:) = xslow(n,:) + stoich_slow(w,:);
99
100                 before = 0;
101                 after = 0;
102
103                 % count how many immigrations are closer to
                        old time, than
104                 % new time
105
106                 for i=1:length(new_I)
107                     if abs(t_old - new_I(i)) < abs(t - new_I(
                            i))
108                         before = before + 1;
109                     else
110                         after = after + 1;
111                     end
112                 end
113
114                 % if all immigrations are closer to new, add
                        all of them to
115                 % new part, otherwise add the ones closer to
                        old time and
116                 % remove them from immi and
117
118                 if before == 0
119                     xslow(n+1,1) = xslow(n+1,1) + after;
120                     % update times of immigration
121                     times_I = times_I(times_I>t);
122                     % update n
123                     n = n+1;
124                 else
125                     xslow(n,1) = xslow(n,1) + before;
126                     xslow(n+1,:) = [0 0];
127                     t = t_old;
128                     times_I = times_I(times_I>new_I(before));
129                 end
130
131             else
132                 t = tlast;
133             end
134
135         end
136
137     % part after more than 'level' cells again
```

```
138     % deterministic, but then for full model.
139
140     x_stoch = xslow(tSAVE>0,:);
141     t_stoch = tSAVE(tSAVE>0);
142
143     % if the end time is already reached in the stochastic
            part, we do
144     % not have to add an other deterministic part.
145
146     if isempty(t_stoch)
147         tnow = t0;
148         xnow = X0;
149     else
150         tnow = t_stoch(end);
151         xnow = [transpose(floor(deval(sol,tnow))) x_stoch(end
                ,:)];
152         if xnow(1) ==1
153             xnow(1) = 0;
154         end
155     end
156
157     % otherwise, add the last part deterministicly
158
159     if tnow < tlast
160         options = odeset('RelTol',1e-12,'AbsTol',1e-12);
161         [last_t, last_x] = ode15s(@(t,y) full_model(t,y,
                treatment_eff),[tnow tlast], xnow, options);
162         x_s = [x_stoch; round(last_x(:,5:6))];
163         t_s = [t_stoch; last_t];
164     else
165         t_s = t_stoch;
166         x_s = x_stoch;
167         last_x = [];
168         last_t = [];
169     end
170
171     % put fast parts togheter
172     t_f1= sol.x(sol.x<tnow);
173     x_f1 = sol.y(:,sol.x<tnow);
174
175     if isempty(last_x)
176         t_f = [t_f1(t_f1>t0)];
177         x_f = [transpose(x_f1(:,t_f1>t0))];
178     else
179         t_f = [t_f1(t_f1>t0) transpose(last_t)];
180         x_f = [transpose(x_f1(:,t_f1>t0)); last_x(:,1:4)];
181     end
182
183     % check if output is in correct format
184     z = size(t_f);
185
```

```
    if z(1)>z(2)
        t_f = transpose(t_f);
    end

end
```

B.2 Code for between host model

BETWEEN models the between host model. The outputs are in the same order as in the code; the final time of the epidemic, the number of susceptibles in time, infections with sensitive type in time, infections with resistant type in time, total number of resistant infections, total number of infections, total number of elderly infections and the total number of infections which are elderly and resistant.

```
function [time_final, S, Is, Ir, num_res, num_tot, num_E,
    num_E_r,p] = ...
    BETWEEN(C, Sinit, init_type, kop, vac_rate, p_eff, G,s)
% LOAD DATABASE OF PATIENTS and a and b value to find r0

% kop is number of patients available in the database.
    vac_rate is a vector
% indicating the probability that a patient in a category is
    vaccinated
% and p_eff that the vaccination is actually working.

load('h_l.mat')

[C1, ~] = size(C);

maxlength = 500;

type = zeros(maxlength,1);
sen = zeros(maxlength,1);
res = zeros(maxlength,1);
time = zeros(maxlength,1);
time_end = zeros(maxlength,1);

Stot = Sinit;

count = 1;
total = 1;

T = 1:1:1*10^6;
sensitive = zeros(length(T),1);
resistant = zeros(length(T),1);

type(1) = init_type; % Pick initial time
sen(1) = 100; % infected with 100 sensitive cells
res(1) = 0;
time(1) = 0;
```

```
34
35 num_res = 0;
36 num_tot = 0;
37 num_E = 0;
38 num_E_r = 0;
39
40 num_vac = vac_rate.*Sinit;
41
42 while count <= total && sum(Stot)
43
44     w = ceil(rand(1,1)*kop);
45
46
47     if type(count) == 1 && sen(count) == 100
48         a = binornd(1,s);
49         if a == 0
50             load(['Data',num2str(w),'.mat'])
51             tf = data(1).tfE_s{1};
52             xf  = data(1).xfE_s{1};
53             ts = data(1).tsE_s{1};
54             xs  = data(1).xsE_s{1};
55         elseif a == 1
56             load(['Data',num2str(w+G(1)-1),'.mat'])
57             tf = data(1).tfE_s_t{1};
58             xf  = data(1).xfE_s_t{1};
59             ts = data(1).tsE_s_t{1};
60             xs  = data(1).xsE_s_t{1};
61         end
62         num_tot = num_tot + 1;
63         num_E = num_E+1;
64     elseif type(count) == 1 && res(count) == 100
65         load(['Data',num2str(w),'.mat'])
66         tf = data(1).tfE_r{1};
67         xf  = data(1).xfE_r{1};
68         ts = data(1).tsE_r{1};
69         xs  = data(1).xsE_r{1};
70         num_res = num_res + 1;
71         num_tot = num_tot + 1;
72         num_E = num_E + 1;
73         num_E_r = num_E_r + 1;
74     elseif type(count) > 1 && sen(count) == 100
75         load(['Data',num2str(w),'.mat'])
76         tf = data(1).tfH_s{1};
77         xf  = data(1).xfH_s{1};
78         ts = data(1).tsH_s{1};
79         xs  = data(1).xsH_s{1};
80         num_tot = num_tot + 1;
81     elseif type(count) > 1 && res(count) == 100
82         load(['Data',num2str(w),'.mat'])
83         tf = data(1).tfH_r{1};
84         xf  = data(1).xfH_r{1};
```

```
        ts  = data(1).tsH_r{1};
        xs   = data(1).xsH_r{1};
        num_res = num_res + 1;
        num_tot = num_tot + 1;
    end

    % Calculate total amount of shedding during the infection

    [t_total, x_total] = togheter(ts, xs, tf, xf);
    y_tot = trapz(t_total,x_total);
    max_x = max(x_total);

    ending = t_total(find(max_x == x_total):end);
    ending_x = x_total(find(max_x == x_total):end);
    ending = ending(ending_x<1.88*10^6); % arbitrary treshold
        when infection is over

    if isempty(ending)
        time_end(count) = time(count);
    else
        time_end(count) = ending(1)+time(count);
    end

    % Estimate r0

    r0 = HILL(y_tot)*(sum(Stot)/sum(Sinit));

    % Pick number of newly infected

    spread = geornd(1/(r0+1));

    if spread > 0

        % Pick type of newly infected by contact matrix

        i = 1;
        Q = 0;

        while i<=spread && Q == 0

            jan = C(type(count),:).*Stot;
            type(total+i) = randsample(1:C1,1,true,jan);

            %%%%%%%%%%%%%%%%%%%%%%%%%%%%%%
            % Effect of vaccinations %

            P_v = binornd(1,(num_vac(type(total+i))/Stot(type
                (total+i))));

            No = 0;

```

```
134             if P_v == 1
135                 No = binornd(1,p_eff(type(total+i)));
136             end
137
138             if No == 0  % the infection does not take place,
                    because the person was vaccinated.
139                 num_vac(type(total+i)) = num_vac(type(total+i
                        )) - 1;
140                 Stot(type(total+i)) = Stot(type(total+i)) -
                        1;
141             elseif No == 1
142                 type(total+i) = [];
143                 spread = spread - 1;
144                 i = i - 1;
145             end
146
147             %%%%%%%%%%%%%%%%%%%%%%%%%%%%%%%%
148
149             if sum(Stot) < 0                    % cannot allow
                    negative number of susceptibles in a group
150                 Q = 1;
151                 spread = i;
152             else
153                 i = i + 1;
154             end
155         end
156
157         % Pick timing of infected by distribution of
                infectious cells
158
159         % Pick number of initial infected cells by
                distribution of infectious
160         % cells
161
162         time_new = randsample(length(t_total),spread,true,
                HILL(x_total));
163         time_new = sort(t_total(time_new));
164         time(total+1:total+spread) = time_new+time(count);
165
166         p = zeros(spread,1);
167
168         for i=1:spread
169
170             [~,I1] = min(abs(ts - time_new(i)));
171             [~,I2] = min(abs(tf - time_new(i)));
172
173             p(i) = xs(I1,2)/(xs(I1,2)+xf(I2,3));
174
175             r = binornd(1,p(i));
176
177             res(total+i) = (r)*100;
```

```
178             sen(total+i) = (1-r)*100;
179
180         end
181
182     end
183
184     % Add this patient to total amount of sensitive and
        resistant virus
185
186     now1 = (round(time(count)):1:(round(time(count))+floor(tf
        (end))))+1;
187
188     for k = now1
189         [~,I1] = min(abs(k - tf));
190         sensitive(k) = sensitive(k) + xf(I1);
191     end
192
193     now2 = (round(time(count)):1:(round(time(count))+floor(ts
        (end))))+1;
194
195     for k = now2
196         [~,I2] = min(abs(k - ts));
197         resistant(k) = resistant(k) + xs(I2);
198     end
199
200     % update
201     total = total + spread;
202     count = count + 1;
203
204 end
205
206 type = type(type>0);
207 time = time(type>0);
208 time_end = time_end(type>0);
209
210 time_final = zeros(2*length(type),1);
211 S = zeros(2*length(type),C1);
212 Is = zeros(2*length(type),C1);
213 Ir = zeros(2*length(type),C1);
214
215 for i=1:length(type)
216     % save what happens in S
217     S(2*i-1,type(i)) = - 1;
218
219     if sen(i)==100
220     %save what happens in I
221         Is(2*i-1,type(i)) = 1;
222         Is(2*i,type(i)) = -1;
223     elseif res(i)==100
224         Ir(2*i-1,type(i)) = 1;
225         Ir(2*i,type(i)) = -1;
```

```
226     end
227
228     % save times of infection i in time_final
229     time_final(2*i-1) = time(i);
230     time_final(2*i) = time_end(i);
231 end
232
233 [time_final, Index] = sort(time_final);
234 Is = Is(Index,:);
235 Ir = Ir(Index,:);
236 S = S(Index,:);
237
238 Is_final = zeros(length(type)*2,C1);
239 Ir_final = zeros(length(type)*2,C1);
240 S_final = zeros(length(type)*2,C1);
241
242 S(1,:) = S(1,:) + Sinit;
243
244 for i=1:length(time_final)
245     for j=1:C1
246         Is_final(i,j) = sum(Is(1:i,j));
247         Ir_final(i,j) = sum(Ir(1:i,j));
248         S_final(i,j) = sum(S(1:i,j));
249     end
250 end
251
252 Is = Is_final;
253 Ir = Ir_final;
254 S = S_final;
255
256 end
```

Bibliography

Baccam, Prasith et al. (2006). "Kinetics of influenza A virus infection in humans". In: *Journal of virology* 80.15, pp. 7590–7599.

Bouvier, Nicole M and Peter Palese (2008). "The biology of influenza viruses". In: *Vaccine* 26, pp. D49–D53.

Cox, RJ, KA Brokstad, and PL Ogra (2004). "Influenza virus: immunity and vaccination strategies. Comparison of the immune response to inactivated and live, attenuated influenza vaccines". In: *Scandinavian journal of immunology* 59.1, pp. 1–15.

Darvishian, Maryam et al. (2017). "Influenza Vaccine Effectiveness in the Netherlands from 2003/2004 through 2013/2014: The Importance of Circulating Influenza Virus Types and Subtypes". In: *PloS one* 12.1, e0169528.

Diekmann Odo, Heesterbeek Hans and Tom Britton (2012). *Princeton Series in Theoretical and Computational Biology : Mathematical Tools for Understanding Infectious Disease Dynamics*. Princeton, US: Princeton University Press.

Disease Control, Center for and Prevention (2009). "Updated Interim Recommendations for the Use of Antiviral Medications in the Treatment and Prevention of Influenza for the 2009-2010 Season". In: URL: http://www.cdc.gov/flu/.

Drake, John W (1993). "Rates of spontaneous mutation among RNA viruses." In: *Proceedings of the National Academy of Sciences* 90.9, pp. 4171–4175.

Driessche, Pauline Van den and James Watmough (2002). "Reproduction numbers and sub-threshold endemic equilibria for compartmental models of disease transmission". In: *Mathematical biosciences* 180.1, pp. 29–48.

Ferguson, Neil M et al. (2003). "A population-dynamic model for evaluating the potential spread of drug-resistant influenza virus infections during community-based use of antivirals". In: *Journal of Antimicrobial Chemotherapy* 51.4, pp. 977–990.

Fiore, Anthony E et al. (2010). *Prevention and control of influenza with vaccines: recommendations of the Advisory Committee on Immunization Practices (ACIP), 2010*. Department of Health, Human Services, Centers for Disease Control, and Prevention.

Fraser, Christophe et al. (2009). "Pandemic potential of a strain of influenza A (H1N1): early findings". In: *Science* 324.5934, pp. 1557–1561.

Frise, Rebecca et al. (2016). "Contact transmission of influenza virus between ferrets imposes a looser bottleneck than respiratory droplet transmission allowing propagation of antiviral resistance". In: *Scientific Reports* 6.

Gillespie, Daniel T (1977). "Exact stochastic simulation of coupled chemical reactions". In: *The journal of physical chemistry* 81.25, pp. 2340–2361.

Gross, Peter A et al. (1995). "The efficacy of influenza vaccine in elderly persons: a meta-analysis and review of the literature". In: *Annals of Internal medicine* 123.7, pp. 518–527.

Gubareva, Larisa V, Laurent Kaiser, and Frederick G Hayden (2000). "Influenza virus neuraminidase inhibitors". In: *The Lancet* 355.9206, pp. 827–835.

Gubareva, LV et al. (1996). "Characterization of mutants of influenza A virus selected with the neuraminidase inhibitor 4-guanidino-Neu5Ac2en." In: *Journal of Virology* 70.3, pp. 1818–1827.

Hadjichrysanthou, Christoforos et al. (2016). "Understanding the within-host dynamics of influenza A virus: from theory to clinical implications". In: *Journal of The Royal Society Interface* 13.119, p. 20160289.

Handel, Andreas, Ira M Longini, and Rustom Antia (2009). "Antiviral resistance and the control of pandemic influenza: the roles of stochasticity, evolution and model details". In: *Journal of theoretical biology* 256.1, pp. 117–125.

Handel, Andreas, Ira M Longini Jr, and Rustom Antia (2007). "Neuraminidase inhibitor resistance in influenza: assessing the danger of its generation and spread". In: *PLoS Computational Biology* 3.12, e240.

Handel, Andreas et al. (2013). "A multi-scale analysis of influenza A virus fitness trade-offs due to temperature-dependent virus persistence". In: *PLoS Comput Biol* 9.3, e1002989.

Holland, John et al. (1982). "Rapid evolution of RNA genomes". In: *Science* 215.4540, pp. 1577–1585.

Hurt, Aeron C et al. (2010). "Assessing the viral fitness of oseltamivir-resistant influenza viruses in ferrets, using a competitive-mixtures model". In: *Journal of virology* 84.18, pp. 9427–9438.

Isin, Basak, Pemra Doruker, and Ivet Bahar (2002). "Functional motions of influenza virus hemagglutinin: a structure-based analytical approach". In: *Biophysical journal* 82.2, pp. 569–581.

Jordan, CDC/ Douglas (2014). *Antigenic Characterization*. URL: https://www.cdc.gov/flu/professionals/laboratory/antigenic.htm (visited on 05/17/2017).

Khodadad, Nastaran et al. (2015). "Prevalence of Influenza A (H1N1) pdm09 Virus Resistant to Oseltamivir in Shiraz, Iran, During 2012-2013". In: *Jundishapur journal of microbiology* 8.8.

Lambert, Nathaniel D et al. (2012). "Understanding the immune response to seasonal influenza vaccination in older adults: a systems biology approach". In: *Expert review of vaccines* 11.8, pp. 985–994.

Mai-Phuong, Hoang Vu et al. (2013). "Oseltamivir resistance among influenza viruses: surveillance in northern Viet Nam, 2009–2012". In: *Western Pacific surveillance and response journal: WPSAR* 4.2, p. 25.

McElhaney, Janet E et al. (2012). "The unmet need in the elderly: how immunosenescence, CMV infection, co-morbidities and frailty are a challenge for the development of more effective influenza vaccines". In: *Vaccine* 30.12, pp. 2060–2067.

Medicine, Institute of (1997). *Vaccine Safety Forum: Summaries of Two Workshops*. Washington, DC: The National Academies Press.

Meijer, Adam et al. (2011). "Oseltamivir-resistant pandemic A (H1N1) 2009 influenza viruses detected through enhanced surveillance in the Netherlands, 2009–2010". In: *Antiviral research* 92.1, pp. 81–89.

Meltzer, Martin I, Nancy J Cox, Keiji Fukuda, et al. (1999). "The economic impact of pandemic influenza in the United States: priorities for intervention". In: *Emerging infectious diseases* 5, pp. 659–671.

Moscona, Anne (2005). "Neuraminidase inhibitors for influenza". In: *New England Journal of Medicine* 353.13, pp. 1363–1373.

Nobusawa, Eri and Katsuhiko Sato (2006). "Comparison of the mutation rates of human influenza A and B viruses". In: *Journal of virology* 80.7, pp. 3675–3678.

Paradis, Eric G et al. (2015). "Impact of the H275Y and I223V mutations in the neuraminidase of the 2009 pandemic influenza virus in vitro and evaluating experimental reproducibility". In: *PloS one* 10.5, e0126115.

Pop-Vicas, A and S Gravenstein (2010). "Influenza in the elderly–A mini-review". In: *Gerontology* 57.5, pp. 397–404.

Racaniello, V. (2009). *Influenza virus transmission*. URL: http://www.virology.ws/2009/04/29/influenza-virus-transmission/ (visited on 05/17/2017).

Salomon, Rachelle and Robert G Webster (2009). "The influenza virus enigma". In: *Cell* 136.3, pp. 402–410.

Samji, Tasleem (2009). "Influenza A: understanding the viral life cycle". In: *Yale J Biol Med* 82.4, pp. 153–159.

Sellke, Thomas (1983). "On the asymptotic distribution of the size of a stochastic epidemic". In: *Journal of Applied Probability* 20.2, pp. 390–394.

Treanor, John (2004). "Influenza vaccine—outmaneuvering antigenic shift and drift". In: *New England Journal of Medicine* 350.3, pp. 218–220.

Viboud, Cécile and Lone Simonsen (2012). "Global mortality of 2009 pandemic influenza A H1N1". In: *The Lancet infectious diseases* 12.9, pp. 651–653.

Xiao, Yanyu, Fred Brauer, and Seyed M Moghadas (2016). "Can treatment increase the epidemic size?" In: *Journal of mathematical biology* 72.1-2, pp. 343–361.